NASA TECHNICAL NOTE

NASA TN D-6579

NASA TN D-6579

DETERMINATION OF STABILITY DERIVATIVES FROM FLIGHT DATA USING A NEWTON-RAPHSON MINIMIZATION TECHNIQUE

by Kenneth W. Iliff and Lawrence W. Taylor, Jr.

Flight Research Center
Edwards, Calif. 93523

NATIONAL AERONAUTICS AND SPACE ADMINISTRATION • WASHINGTON, D. C. • MARCH 1972

1. Report No.	2. Government Accession No.	3. Recipient's Catalog No.
NASA TN D-6579		

4. Title and Subtitle	5. Report Date
DETERMINATION OF STABILITY DERIVATIVES FROM FLIGHT DATA USING A NEWTON-RAPHSON MINIMIZATION TECHNIQUE	March 1972
	6. Performing Organization Code

7. Author(s)	8. Performing Organization Report No.
Kenneth W. Iliff and Lawrence W. Taylor, Jr.	H-626
	10. Work Unit No. 126-62-01-02-24

9. Performing Organization Name and Address	11. Contract or Grant No.
NASA Flight Research Center P. O. Box 273 Edwards, California 93523	
	13. Type of Report and Period Covered: Technical Note

12. Sponsoring Agency Name and Address	14. Sponsoring Agency Code
National Aeronautics and Space Administration Washington, D. C. 20546	

15. Supplementary Notes

16. Abstract

A modified Newton-Raphson or quasilinearization minimization technique for determining stability derivatives from flight data was developed and compared with simple-equations, analog-matching, least-squares, and Shinbrot methods of analysis. For the data analyzed, the solutions computed by using the estimates obtained from the Newton-Raphson technique fit the data and determined coefficients adequately. A further modification to include a priori information was found to be useful.

A model statistically similar to the flight data was analyzed using the same methods (excluding analog matching), and the Newton-Raphson technique was found to yield superior estimates. An approximate Cramèr-Rao bound was compared with the error covariance matrix of the model and was found to provide information about the reliability of the individual estimates obtained.

The technique was successfully applied to data obtained from a light airplane, a large supersonic airplane, and a lifting body vehicle. It was shown that the reliability of the estimates of a given coefficient obtained from these vehicles depends upon the data analyzed.

17. Key Words (Suggested by Author(s))	18. Distribution Statement
Identification Nonlinear minimization Stability derivative determination	Unclassified - Unlimited

19. Security Classif. (of this report)	20. Security Classif. (of this page)	21. No. of Pages	22. Price*
Unclassified	Unclassified	57	$3.00

*For sale by the National Technical Information Service, Springfield, Virginia 22151

DETERMINATION OF STABILITY DERIVATIVES FROM FLIGHT DATA USING A NEWTON-RAPHSON MINIMIZATION TECHNIQUE

Kenneth W. Iliff and Lawrence W. Taylor, Jr.
Flight Research Center

INTRODUCTION

Identifying a system which will accurately and reliably determine the stability and control derivatives (i.e., coefficients of the differential equations of motion) of airplanes from flight data remains difficult and time consuming, despite the considerable effort that has been devoted to it over the years. There is no lack of methods to determine stability derivatives from flight data; on the contrary, many methods have been tried, and under idealized conditions most have been successful. Unfortunately, however, inadequate aircraft excitation, instrumentation and measurement noise, and departures of the actual airplane from the model used for the airplane dynamics generally cause considerable error in the resulting estimates.

Among the methods available to solve this problem, the simplified-equations, time-vector (ref. 1), analog-matching (refs. 1 and 2), and regression methods (refs. 3 and 4) have been used most extensively. The simplified-equations and time-vector methods are often severely limited because the set of aerodynamic coefficients obtainable is incomplete and the types of applicable responses are restricted. The analog-matching method is also limited because estimates resulting from it vary with the skill and technique of the operator. The accuracy of the coefficients estimated by the regression methods is unreliable if measurement noise on the response is excessive or maneuvers are poorly conditioned.

Of most interest is the possibility of obtaining a linear model which results in a computed response that best fits the measured data. Analog matching imitates this approach, but the estimates reflect the operator's judgment. Regression methods minimize the integral-squared error in fitting the measured data to a linear model of the system point by point in an algebraic sense, ignoring the time-sequential nature of the aircraft and model responses. Many of these difficulties can be circumvented intuitively by minimizing the weighted integral-squared error of the difference between the computed and measured response. The standard gradient technique (ref. 5) can be used for this minimization, but this technique has been found to converge much too slowly. Consequently, a modified form of the Newton-Raphson technique (ref. 5) was investigated as a means of obtaining more rapid convergence. This method could also be viewed as an application of quasi-linearization (ref. 6).

This report compares the results obtained by using the modified Newton-Raphson technique of minimization with the results obtained from simplified-equations, analog-matching, and regression methods for a representative lateral-directional flight maneuver. The proposed method is applied to obtain stability and control

derivatives for vehicles encompassing the geometric and flight extremes of modern aircraft. An example of the application of the method to the longitudinal equations of motion of an airplane is also presented.

SYMBOLS

Physical quantities in this report are given in the International System of Units (SI) and parenthetically in U. S. Customary Units. The measurements were taken in U. S. Customary Units. Factors relating the two systems are presented in reference 7.

A	stability matrix $(P \times P)$
$A a_{ij}$	null matrix except for the i-jth element which equals 1 $(P \times P)$
A_i	ith row of the stability matrix $(1 \times P)$
a_{ij}	i-jth element of A
a_x, a_y, a_z	linear acceleration along the X-, Y-, and Z-axes, respectively, g units
B	control matrix $(P \times Q)$
$B b_{ij}$	null matrix except for the i-jth element which equals 1 $(P \times Q)$
B_i	ith row of the control matrix $(1 \times Q)$
b_{ij}	i-jth element of B
C	augmented A and B matrices $(P \times (P + Q))$
C_i	ith row of the C matrix $(1 \times (P + Q))$
$\mathbf{c}$	vector of unknown coefficients $(m \times 1)$
c_i	ith element of the c vector
$\mathbf{c}_0$	vector of a priori estimates of the unknown coefficients $(m \times 1)$
$\mathbf{c}_T$	vector of actual values of unknown coefficients $(m \times 1)$
D_1	weighting matrix for observation vector $(R \times R)$

D_2	weighting matrix for a priori estimate vector (m × m)
$d_{1_{ij}}, d_{2_{ij}}$	i-jth elements of D_1 and D_2, respectively
$E\{\cdot\}$	expected value
$\hat{F}$	matrix functional of $\hat{z}$ for Shinbrot method ($l \times (R-P)$)
F_s	matrix functional of z_s for Shinbrot method ($l \times P$)
f	method function vector ($l \times 1$)
f_j	jth element of method function vector
G	partition of matrix relating the state vector to the observation vector ((R-P) × P)
g	acceleration due to gravity, m/sec^2 (ft/sec^2)
g	vector of observation biases (R × 1)
g_i	ith element of g
H	partition of matrix relating the control vector to the observation vector ((R-P) × Q)
$\hat{h}$	vector functional of $\hat{z}$ for modified least-squares method ((R-P) × 1)
h_s	vector functional of z_s for modified least-squares method (P × 1)
h_u	vector functional of u for modified least-squares method (Q × 1)
I	identity matrix
J	cost functional or weighted mean-square-fit error
K	scalar weighting factor (gain) for a priori weighting matrix
L	rolling moment divided by the moment of inertia about the X-axis, rad/sec^2
l	number of time samples

M	pitching moment divided by the moment of inertia about the Y-axis, rad/sec^2
m	number of unknowns in **c** vector
N	yawing moment divided by the moment of inertia about the Z-axis, rad/sec^2
n	vector of measurement noise ($R \times 1$)
n_i	i^{th} element of **n**
P	number of state variables
p	roll rate, rad/sec or deg/sec
Q	number of control variables
q	pitch rate, rad/sec or deg/sec
R	number of observation variables
r	yaw rate, rad/sec or deg/sec
T	total time, sec
t	intermediate or incremental time, sec
tr	matrix trace operation (sum of diagonal elements)
u	control vector ($Q \times 1$)
V	velocity, m/sec (ft/sec)
W	covariance matrix of the noise
X	longitudinal force divided by mass, m/sec^2 (ft/sec^2)
x	state vector ($P \times 1$)
x_i, x_j	i^{th} and j^{th} component of **x**
Y	side force divided by mass and velocity, rad/sec
y	observation vector ($R \times 1$)
y_i	i^{th} element of the **y** vector
Z	normal force divided by mass and velocity, rad/sec

$\mathbf{z}_s$	measurement of state variables (P × 1)
$\hat{\mathbf{z}}$	measurement related to derivatives of state variables ((R-P) × 1)
$\mathbf{z}$	measurement of observation vector (R × 1)
α	angle of attack of X-axis, rad or deg
α_0	angle of attack of principal X-axis, rad
β	angle of sideslip, rad or deg
Γ_s	weighting matrix for $\mathbf{h}_s$ used in modified least-squares method (P × P)
Γ_u	weighting matrix for $\mathbf{h}_u$ used in modified least-squares method (Q × Q)
Δ	increment
δ	first variation
δ_a	aileron deflection, rad or deg
δ_e	elevator deflection, rad or deg
δ_r	rudder deflection, rad or deg
δ_0	constant control deflection, rad or deg
ϵ	relaxation coefficient
ζ	damping ratio
Θ	pitch angle, rad or deg
$\rho(\cdot)$	probability density function of $(\cdot)$
$\sigma^2_{a_{ij}}$	approximate estimate for the variance determined with the Cramèr-Rao inequality of the i-jth term
σ^2_{ij}	estimated variance of wind-tunnel estimates for the i-jth element of D_2
σ^2_{CR}	estimate for the variance determined with the Cramèr-Rao inequality
σ^2_E	variance of the estimates from an experimental model

τ	auxiliary time variable, sec
Φ	Cramèr-Rao bound for the error covariance matrix
φ	bank angle, rad or deg
ω	frequency, rad/sec
$\nabla_{\mathbf{c}}(\cdot)$	gradient of $(\cdot)$ with respect to $\mathbf{c}$
$\nabla_{\mathbf{g}}(\cdot)$	gradient of $(\cdot)$ with respect to $\mathbf{g}$

Subscripts:

d	Dutch roll
e	extended
i	i^{th} row or component
j	j^{th} column or component
k	iteration index
me	measured
0	a nominal or constant value
$\delta_a, \delta_r, \delta_e, \delta_0$, p, q, r, V, α, β, φ, Θ	partial derivatives with respect to subscripted variables

Superscripts:

i, j	index representing time of sample
T	matrix transpose

A dot over a quantity denotes the time derivative of that quantity. Principal axes are used throughout.

Boldface type indicates a vector.

STABILITY-DERIVATIVE DETERMINATION

The task of determining all the stability and control derivatives can be greatly simplified if it is realized that some of the dynamic modes may be uncoupled for most aircraft configurations. The longitudinal modes are usually separated from the lateral-directional modes because the resulting error is small. The bulk of this report

deals with the lateral-directional modes, because this estimation problem is more complex than that for the longitudinal modes. After the proposed technique is fully developed and evaluated for the lateral-directional modes, an example is given to show that the method is equally successful for a longitudinal mode.

The model most often used to describe lateral-directional airplane dynamics can be expressed as a system of linear, constant-coefficient, differential equations in the following form (refs. 8 and 9):

$$\dot{\mathbf{x}}(t) = A\mathbf{x}(t) + B\mathbf{u}(t) \tag{1}$$

where

$$\mathbf{u}(t) = \begin{bmatrix} \delta_a(t) \\ \delta_r(t) \\ \delta_0(t) \end{bmatrix} \qquad \mathbf{x}(t) = \begin{bmatrix} p(t) \\ r(t) \\ \beta(t) \\ \varphi(t) \end{bmatrix} \qquad \dot{\mathbf{x}}(t) = \begin{bmatrix} \dot{p}(t) \\ \dot{r}(t) \\ \dot{\beta}(t) \\ \dot{\varphi}(t) \end{bmatrix}$$

$$A = \begin{bmatrix} L_p & L_r & L_\beta & 0 \\ N_p & N_r & N_\beta & 0 \\ \alpha_0 & -1 & Y_\beta & Y_\varphi \\ 1 & 0 & 0 & 0 \end{bmatrix} \qquad B = \begin{bmatrix} L_{\delta_a} & L_{\delta_r} & L_{\delta_0} \\ N_{\delta_a} & N_{\delta_r} & N_{\delta_0} \\ Y_{\delta_a} & Y_{\delta_r} & Y_{\delta_0} \\ 0 & 0 & 0 \end{bmatrix}$$

It should be noted that no state noise is considered in this analysis. The last column in the B matrix represents the effect of an uncertain bias on $\dot{p}$, $\dot{r}$, and $\dot{\beta}$.

Next $\mathbf{z}_S(t)$ and $\hat{\mathbf{z}}(t)$ are defined as the noise-contaminated measurements of $\mathbf{x}(t)$ and $\dot{\mathbf{x}}(t)$, respectively; that is, $\mathbf{z}_S(t)$ is the noise-contaminated measurement of the state vector $\mathbf{x}(t)$, $\hat{\mathbf{z}}(t)$ is the noise-contaminated measurement of $\dot{\mathbf{x}}(t)$, and the control inputs $\mathbf{u}(t)$ are considered to be noise-free. For the remainder of this report, the time argument of the variables is omitted where the time dependence is clear.

The problem addressed is: Given $\mathbf{z}_S$, $\hat{\mathbf{z}}$, and $\mathbf{u}$, determine certain unknown elements of the A and B matrices. In airplane dynamics these coefficients of the linearized equations of motion are the stability and control derivatives which result from the Taylor's series expansion of the aerodynamic forces and moments.

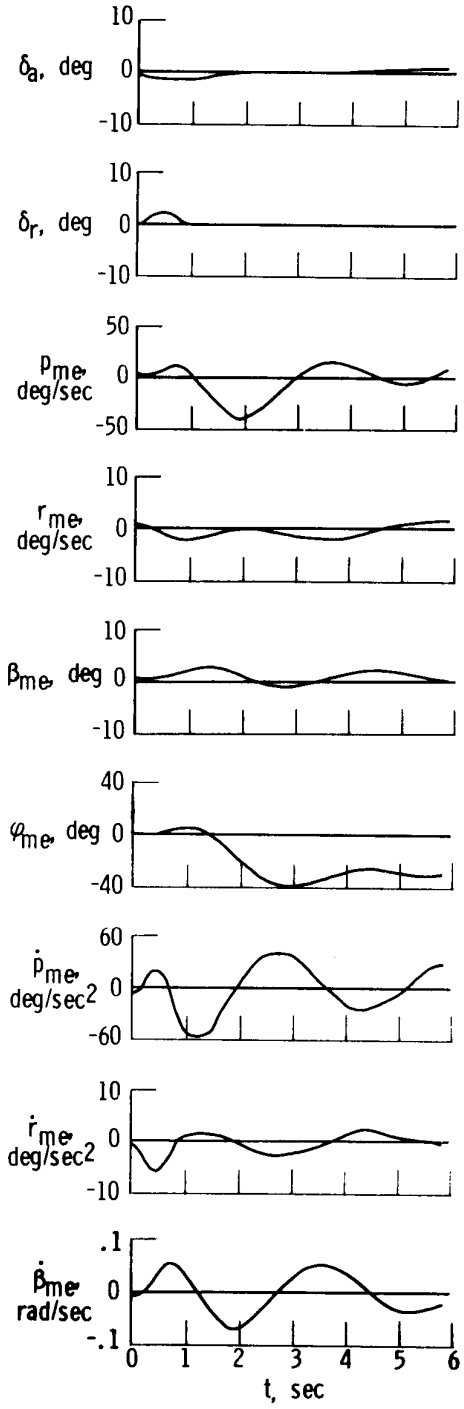

Figure 1. Time history of X-15 maneuver.

REVIEW OF PREVIOUS METHODS

To examine previous methods of determining stability and control derivatives, one typical flight maneuver was selected and several methods were applied to analyze the data obtained from the maneuver. This maneuver was chosen because all the measurement signals appearing in $\mathbf{z}_S$, $\hat{\mathbf{z}}$, and $\mathbf{u}$ were available, which is needed in some methods to estimate all the coefficients. Except for this stipulation, the maneuver was arbitrarily selected and was not known to favor any of the methods.

The maneuver selected was for the X-15 research airplane (ref. 10) at a hypersonic flight condition (figs. 1 to 13). Time histories of the maneuver are shown in figure 1. The control-input time histories apply to all the data in figures 2 to 8, 10, and 12 and therefore are not repeated. The $\dot{\beta}_{me}$ data, which are used in the subsequent analysis, were not measured directly in flight, but were computed from other flight variables by using the following equation:

$$\dot{\beta}_{me} = \alpha p_{me} - r_{me} + \left(a_{y_{me}} + \sin \varphi_{me}\right) \frac{g}{V}$$

The least-squares and Shinbrot methods (discussed later) use $\dot{\beta}_{me}$ because the formulation is more convenient with $\dot{\beta}_{me}$ than with $a_{y_{me}}$ and the resulting estimated parameters are identical.

Stability derivatives are usually determined first from wind-tunnel data. However, because of unavoidable differences between the wind-tunnel test and flight conditions, the wind-tunnel values should be considered only as initial estimates. Figure 2 compares time histories obtained from flight with those computed by using wind-tunnel values. The differences shown offer motivation for determining coefficients from flight data.

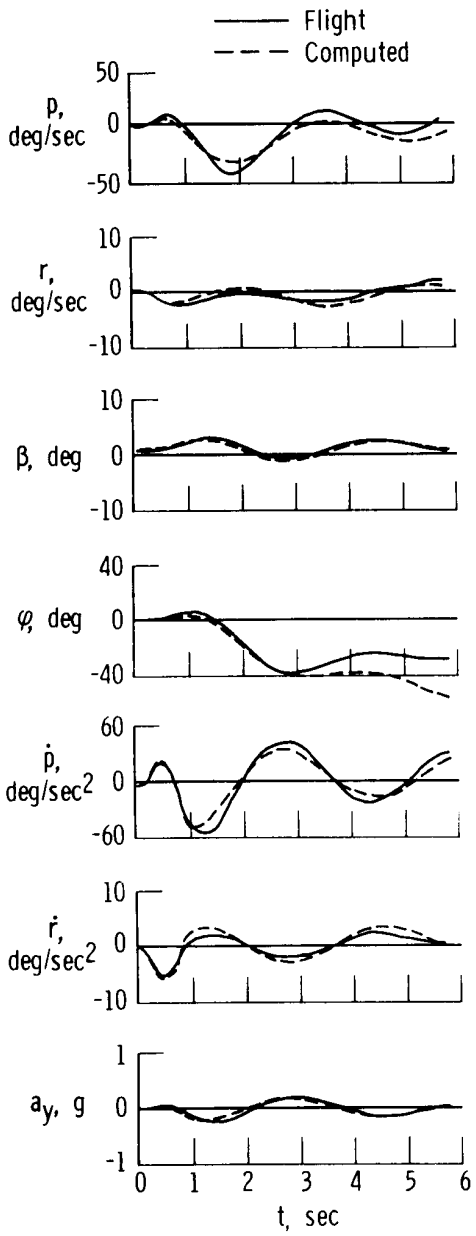

Figure 2. Comparison of X-15 time histories measured in flight and computed by using predictions based upon wind-tunnel tests.

Simplified-Equations Method

For selected types of responses the effect of only a few coefficients dominates, thus permitting the use of simple expressions to determine these coefficients. Some of the expressions (ref. 1) that are used for this purpose and the types of responses that are required are as follows:

$$N_{\delta_r} \approx \frac{\Delta \dot{r}}{\Delta \delta_r} \quad \text{(rudder pulse)}$$

$$L_{\delta_a} \approx \frac{\Delta \dot{p}}{\Delta \delta_a} - L_p \frac{\Delta p}{\Delta \delta_a} \quad \text{(aileron pulse)}$$

$$N_{\delta_a} \approx \frac{\Delta \dot{r}}{\Delta \delta_a} - N_r \frac{\Delta r}{\Delta \delta_a} - N_p \frac{\Delta p}{\Delta \delta_a} - N_\beta \frac{\Delta \beta}{\Delta \delta_a} \quad \text{(aileron pulse)}$$

$$Y_\beta \approx \frac{g}{V} \frac{\Delta a_y}{\Delta \beta} \quad \text{(Dutch roll oscillation)}$$

$$N_\beta \approx \omega_d^2 + \alpha L_\beta \quad \text{(Dutch roll oscillation)}$$

$$L_\beta \approx -L_{\delta_r} \frac{d\delta_r}{d\beta} - L_{\delta_a} \frac{d\delta_a}{d\beta} \quad \text{(steady sideslip)}$$

$$L_p \approx -L_{\delta_a} \frac{\Delta \delta_a}{\Delta p} \quad \text{(aileron step)}$$

$$N_r \approx -2\zeta_d \omega_d - Y_\beta \quad \text{(Dutch roll oscillation)}$$

The notation has been changed from that of reference 1 to be consistent with the principal axes system used in the preceding equations of state. The time-vector method, also discussed in reference 1, serves as a basis for the equations in which oscillatory responses are used.

A partial set of coefficients was obtained by using equations, such as the preceding, from the example set of X-15 flight data. These values (predictions based upon wind-tunnel values were used to complete the set) were substituted into the equations of motion, and time histories were computed. These

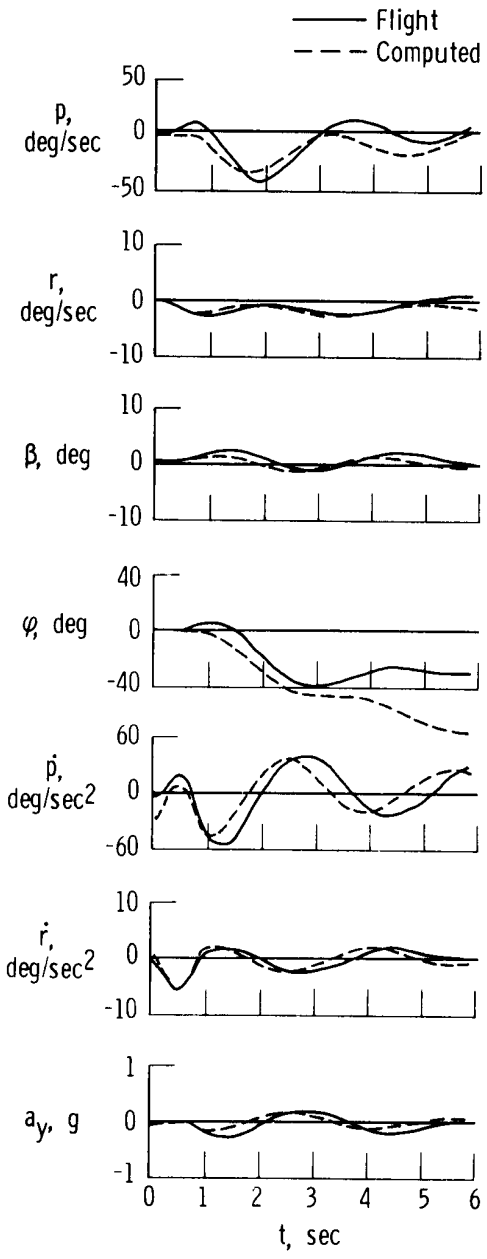

Figure 3. Comparison of X-15 time histories measured in flight and computed by using coefficients obtained from flight data by the method of simple equations.

time histories are compared with those measured in flight in figure 3, which shows differences at least as great as for the time histories computed by using the wind-tunnel coefficients.

Analog-Matching Method

The equations of motion can be readily solved by using an analog computer. This would suggest fitting the measured responses with the computed responses by manually adjusting the potentiometers of the analog computer mechanization, in which the settings correspond to particular values of the coefficients. The operation, referred to as analog matching, is described in detail in references 1 and 2. Analog matching was applied to the X-15 flight data, with the results shown in figure 4. Because analog matching is a manual operation, the operator can somewhat constrain values of some of the coefficients on the basis of his knowledge of the quality of the wind-tunnel values and his experience, that is, a priori information.

By comparing the results shown in figures 3 and 4, it is apparent that the fit has been improved considerably. Nevertheless, it would be desirable to automate the fitting process, perhaps improving it further as well as making it more efficient. Regardless of the method used, the same match can be obtained with analog matching, because it solves the same equations, but the effort involved may be prohibitive.

Least-Squares Method

One approach to determining aerodynamic derivatives is to minimize the integral square of the state equation error by substituting the measured values for the state and its derivatives, that is, minimize the following cost functional:

$$J = \int_0^T \left(\hat{\dot{\mathbf{z}}} - A\mathbf{z}_s - B\mathbf{u}\right)^T \left(\hat{\dot{\mathbf{z}}} - A\mathbf{z}_s - B\mathbf{u}\right) dt \quad (2)$$

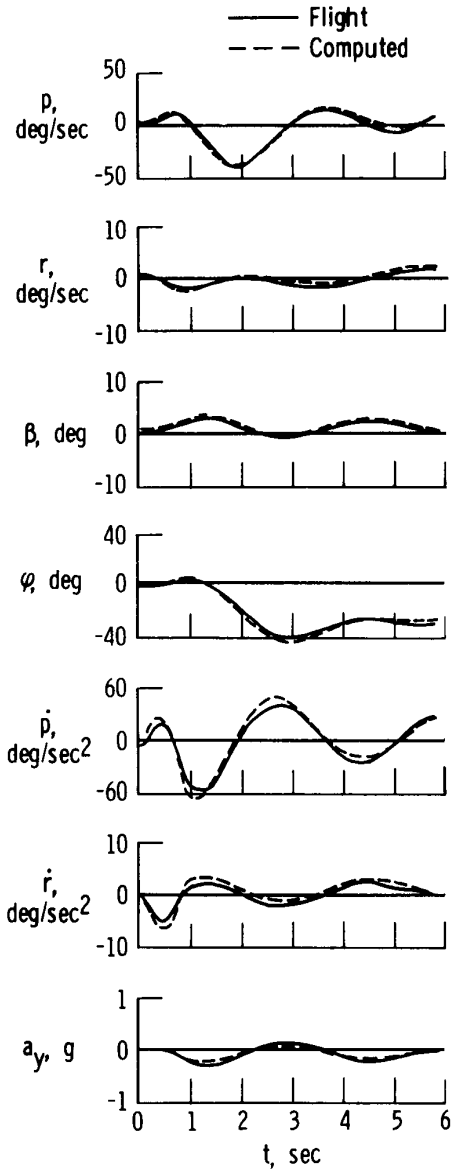

Figure 4. Analog match of X-15 time histories measured in flight.

To derive an expression for the values of A and B that minimizes equation (2), let

$$C = \left[\begin{array}{c|c} A & B \end{array}\right]$$

then

$$J = \int_0^T \left\{ \hat{z}^T\hat{z} - 2\hat{z}^T C\left[-\frac{z_s}{u}-\right] + \left[-\frac{z_s}{u}-\right]^T C^T C\left[-\frac{z_s}{u}-\right] \right\} dt$$

$$= \int_0^T \hat{z}^T\hat{z}\, dt - 2\int_0^T \hat{z}^T C\left[-\frac{z_s}{u}-\right] dt + \int_0^T \left[-\frac{z_s}{u}-\right] C^T C\left[-\frac{z_s}{u}-\right] dt$$

$$= \mathrm{tr}\left[\int_0^T \hat{z}^T\hat{z}\, dt\right] - 2\mathrm{tr}\left\{\int_0^T \left[-\frac{z_s}{u}-\right]\hat{z}^T C\, dt\right\} + \mathrm{tr}\left\{\int_0^T \left[-\frac{z_s}{u}-\right]\left[-\frac{z_s}{u}-\right]^T C^T C\, dt\right\}$$

where

$$\mathrm{tr}(AB) = \mathrm{tr}(BA)$$

The minimization is achieved by taking the first variation of the preceding expression, that is,

$$\delta J = -2\mathrm{tr}\left\{\int_0^T \left[-\frac{z_s}{u}-\right]\hat{z}^T dt\, \delta C\right\} + 2\mathrm{tr}\left\{\int_0^T \left[-\frac{z_s}{u}-\right]\left[-\frac{z_s}{u}-\right]^T C^T dt\, \delta C\right\}$$

and putting

$$\delta J = 0$$

The resulting solution requires that, for an arbitrary δC,

$$\int_0^T \left\{-\left[-\frac{z_s}{u}-\right]\hat{z}^T dt\right\} + \int_0^T \left[-\frac{z_s}{u}-\right]\left[-\frac{z_s}{u}-\right]^T C^T dt = 0$$

Then

$$C^T = \left\{\int_0^T \left[-\frac{z_s}{u}-\right]\left[-\frac{z_s}{u}-\right]^T dt\right\}^{-1} \int_0^T \left[-\frac{z_s}{u}-\right]\hat{z}^T dt \qquad (3)$$

This equation is the solution to the least-squares problem. It has the advantage of a compact form, but it disguises the independence of each of the equations to be minimized. This limitation can be illustrated in the following manner. Considering only the first state equation and minimizing the same cost functional,

$$J = \int_0^T \left(\dot{p}_{me} - L_p p_{me} - L_r r_{me} - L_\beta \beta_{me} - L_{\delta_a} \delta_a - L_{\delta_r} \delta_r - L_{\delta_0} \delta_0 \right)^2 dt$$

where the subscript me identifies the measured value. A more convenient form may be obtained by making the following substitutions:

$$A_1 = \begin{bmatrix} L_p & L_r & L_\beta & 0 \end{bmatrix}$$

$$B_1 = \begin{bmatrix} L_{\delta_a} & L_{\delta_r} & L_{\delta_0} \end{bmatrix}$$

$$C_1 = \left[A_1 \,\vdots\, B_1 \right]$$

Then

$$J = \int_0^T \left\{ \dot{p}_{me} - C_1^T \begin{bmatrix} z_s \\ \overline{u} \end{bmatrix} \right\}^2 dt$$

Once again taking the first variation and setting the resulting expression equal to zero gives

$$C_1^T = \left\{ \int_0^T \begin{bmatrix} z_s \\ \overline{u} \end{bmatrix} \begin{bmatrix} z_s \\ \overline{u} \end{bmatrix}^T dt \right\}^{-1} \int_0^T \dot{p}_{me} \begin{bmatrix} z_s \\ \overline{u} \end{bmatrix} dt$$

Now C_1 is the first row of the C matrix, and $\dot{p}_{me}$ is the first element of $\hat{\dot{z}}$, which makes it apparent that the elements of the first row of the C matrix are independent of all the elements of $\hat{\dot{z}}$ except the first, $\dot{p}_{me}$. A similar relationship is easily shown for the other rows of the C matrix. This independence is one of the drawbacks of the least-squares method, in that only one of the measured state derivatives is used in determining a given row of the C matrix. If one of the signals has not been measured, the least-squares method does not provide an estimate of the derivatives related to that signal. This independence also illustrates that the estimate of one row of the C matrix is obtained independently of the other rows, and no "trade-off" can be made between elements in different rows to improve the match.

Figure 5 shows the fit of $\dot{p}$, $\dot{r}$, and $\dot{\beta}$ obtained with the least-squares method. The fit is considered to be good. Since only $\dot{p}$, $\dot{r}$, and $\dot{\beta}$ were fit, these are the only time histories shown. It should be noted that the fit of the time histories is not a solution of the differential equations of motion. It is merely a minimization of the integral-squared error of the fit of the measured data to a linear model of the system (that is, point by point in an algebraic sense, ignoring the time-sequential nature of the data). In other words, only measured state variables and their derivatives are

used in the minimization because the differential equations are never solved for the computed state.

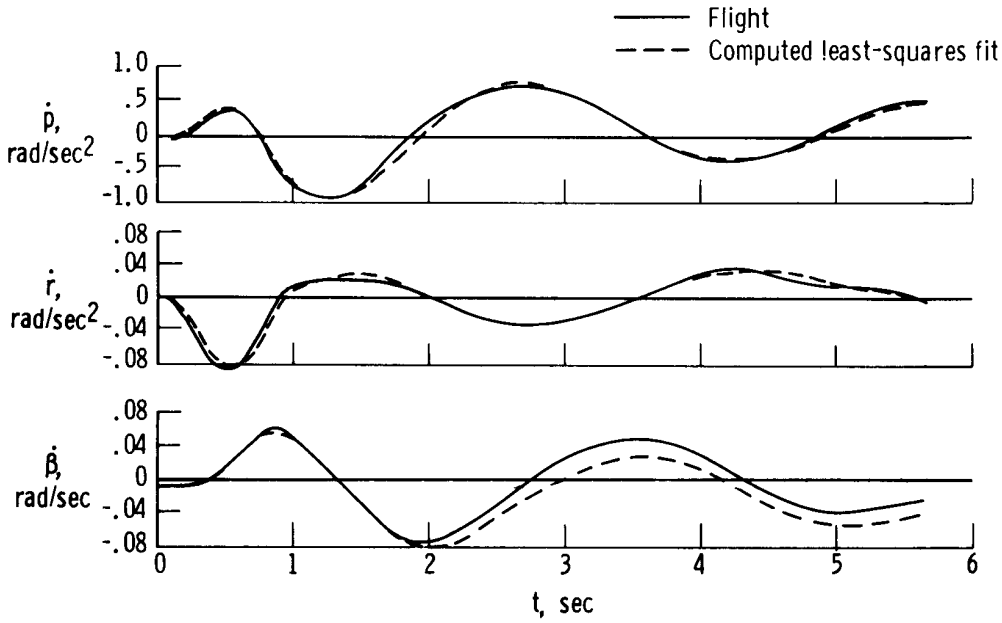

Figure 5. Least-squares fit of X-15 flight time histories.

The least-squares values of the coefficients were substituted into the A and B matrices, and a time history was computed and compared, in figure 6, with that measured in flight. The fit of $\dot{p}$, $\dot{r}$, and $\dot{\beta}$ is still good, but other variables have drifted apart, especially φ, p, and r. These are typical results obtained by using the least-squares method. The poor fit of the state variables should not be surprising, inasmuch as the computed solution is not included in the minimization.

Shinbrot Method

In reference 4, Shinbrot showed the existence of similarities in a variety of regression methods and introduced a general method function, f(t). This can be shown by starting with the state equation with the measured values z_s and $\hat{z}$ denoting the state and its derivative, then multiplying by a method function and integrating. Thus

$$\int_0^T \hat{z}(t) f(t)^T dt = C \int_0^T \left[\frac{z_s(t)}{u(t)} \right] f(t)^T dt$$

The method functions used are those suggested by Shinbrot in reference 4 and have the form

$$f_j = \frac{1-\cos\left(\frac{2\pi j t}{T}\right)}{2} \qquad j = 1, 2, \ldots, l$$

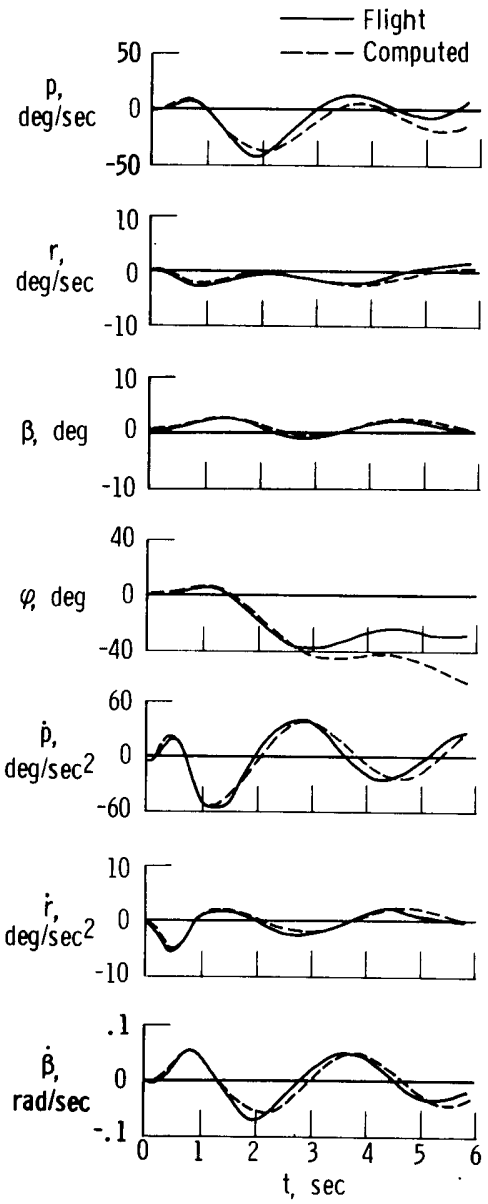

Figure 6. Comparison of X-15 time histories measured in flight and computed by using coefficients obtained from flight data with the least-squares method.

where the maximum of j must be greater than or equal to the number of unknown elements in C. Then define

$$\hat{F}^T = \int_0^T \hat{z}\, f^T\, dt$$

and

$$F_S{}^T = \int_0^T \left[\frac{z_S}{u}\right] f^T\, dt$$

It follows that

$$\hat{F} = F_S\, C^T$$

For this transformation, the solution may be obtained in the form

$$F_S{}^T\, F_S\, C^T = F_S{}^T\, \hat{F}$$

$$C^T = \left[F_S{}^T\, F_S\right]^{-1} F_S{}^T\, \hat{F} \tag{4}$$

It can be readily shown that this method has the same row independence of C illustrated for the least-squares method. This method is similar to the least-squares method and yields nearly identical results, as shown in figure 7, in that the computed time histories also drift away from the measured values.

Modified Least-Squares Method

Some of the difficulties encountered with the least-squares method can be overcome by modifying it to include the state vectors in the error minimization, thus combining the standard least-squares method with the integrated least-squares method. The integrated least-squares method is merely the least-squares formulation with the integral of each of the variables replacing the variables.

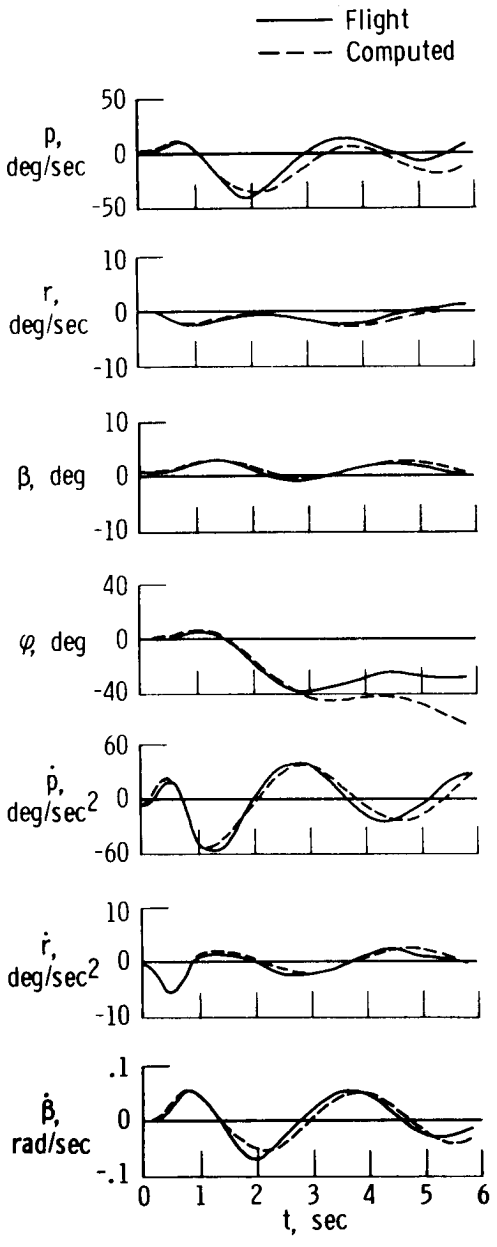

Figure 7. Comparison of X-15 time histories measured in flight and computed by using coefficients obtained from flight data with the Shinbrot method.

By defining

$$\mathbf{h_s}(t) = \Gamma_s \int_0^t \mathbf{z_s}(\tau)\, d\tau + \mathbf{z_s}(t)$$

$$\mathbf{h_u}(t) = \Gamma_u \int_0^t \mathbf{u}(\tau)\, d\tau + \mathbf{u}(t)$$

and

$$\hat{\mathbf{h}}(t) = \int_0^t \hat{\mathbf{z}}(\tau)\, d\tau + \hat{\mathbf{z}}(t)$$

where Γ_s is a (P × P) diagonal matrix and Γ_u is a (Q × Q) diagonal matrix which provide weighting among the various signals representing the relative confidence in the signals, then

$$J = \int_0^T \left\{ \hat{\mathbf{h}} - C \begin{bmatrix} \mathbf{h_s} \\ \hline \mathbf{h_u} \end{bmatrix} \right\}^T \left\{ \hat{\mathbf{h}} - C \begin{bmatrix} \mathbf{h_s} \\ \hline \mathbf{h_u} \end{bmatrix} \right\} dt$$

or the complete formulation for the minimum becomes, as in least squares,

$$\int_0^T \begin{bmatrix} \mathbf{h_s} \\ \hline \mathbf{h_u} \end{bmatrix} \hat{\mathbf{h}}^T dt = \int_0^T \begin{bmatrix} \mathbf{h_s} \\ \hline \mathbf{h_u} \end{bmatrix} \begin{bmatrix} \mathbf{h_s} \\ \hline \mathbf{h_u} \end{bmatrix}^T dt\, C^T \tag{5}$$

$$C^T = \left\{ \int_0^T \begin{bmatrix} \mathbf{h_s} \\ \hline \mathbf{h_u} \end{bmatrix} \begin{bmatrix} \mathbf{h_s} \\ \hline \mathbf{h_u} \end{bmatrix}^T dt \right\}^{-1} \int_0^T \begin{bmatrix} \mathbf{h_s} \\ \hline \mathbf{h_u} \end{bmatrix} \hat{\mathbf{h}}^T dt$$

Once again it is easily shown that this method has the same row independence of C shown by both the least-squares and the Shinbrot method.

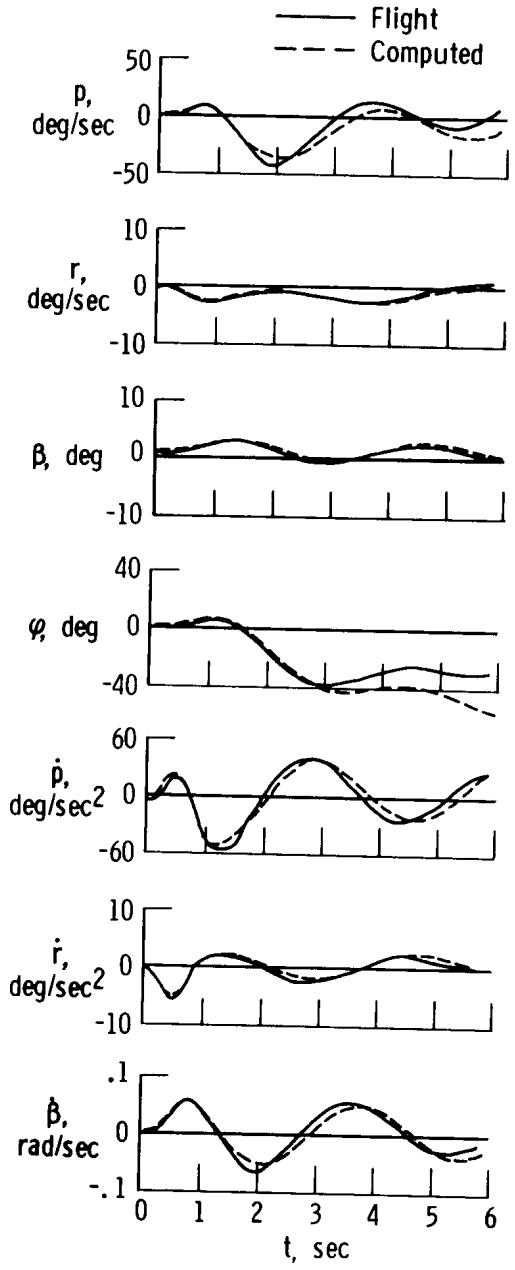

Figure 8. Comparison of X-15 time histories measured in flight and computed by using coefficients obtained from flight data with the modified least-squares method.

The fit of the computed time history to that obtained in flight in figure 8 is still not acceptable. It would, of course, be desirable to minimize the differences in the time histories. Although this can be done, it will be shown that the identification problem becomes nonlinear, requiring some iterative technique.

Modified Newton-Raphson Technique

Once the mathematical model for the system has been selected, two items remain to be specified to identify the system: (1) the cost functional to be minimized, and (2) an algorithm to minimize the cost functional. In some of the methods analyzed these items are not readily specified. In analog matching, the cost functional is obscure in that what constitutes a good fit is primarily a function of the judgment of the operator. The operator minimizes his subjective cost functional by adjusting potentiometers until, in his opinion, the fit is attained. This procedure can be time consuming, and the results vary greatly from operator to operator. The regression methods discussed alleviate some of the problems of analog matching in that a cost functional is specified and is readily minimized because the formulation is linear in the parameters to be estimated. Unfortunately, the resulting fit to the measured data is unsatisfactory. Ultimately, a linear model is desired with a computed response that best fits the measured data. It has been demonstrated that the fit obtained with analog matching is superior to that obtained with the other methods. This suggests that the cost functional should reflect the difference between the computed response based upon the coefficient estimates and the measured response. Therefore, more satisfactory results would be expected if the problem were posed as one of minimizing a quadratic cost functional of this difference. Many other criteria could be proposed, but the quadratic is the most thoroughly analyzed form and has the most desirable mathematical characteristics.

To be more specific, consider the

following model:

$$\dot{\mathbf{x}} = A\mathbf{x} + B\mathbf{u}$$

$$\mathbf{y} = \left[\begin{array}{c} I \\ \hline G \end{array}\right] \mathbf{x} + \left[\begin{array}{c} I \\ \hline H \end{array}\right] \mathbf{u} \tag{6}$$

where A and B are defined as in equation (1) and

$$G = \begin{bmatrix} L_p & L_r & L_\beta & 0 \\ N_p & N_r & N_\beta & 0 \\ 0 & 0 & Y_\beta & 0 \end{bmatrix} \qquad H = \begin{bmatrix} L_{\delta_a} & L_{\delta_r} & L_{\delta_0} \\ N_{\delta_a} & N_{\delta_r} & N_{\delta_0} \\ Y_{\delta_a} & Y_{\delta_r} & Y_{\delta_0} \end{bmatrix}$$

The non-zero elements of G and H are also elements of A and B, respectively. The vector $\mathbf{y}$ is the set of "output" response quantities:

$$\mathbf{y} = \begin{bmatrix} p & r & \beta & \varphi & \dot{p} & \dot{r} & a_y \end{bmatrix}^T$$

Let $\mathbf{z}$ denote the measurement of the actual aircraft response quantities corresponding to $\mathbf{y}$. Although no state noise is assumed, $\mathbf{z}$ would not be exactly the same as $\mathbf{y}$ because of measurement errors and differences between the actual and the assumed linear model (eq. (6)). A reasonable description of the relationship of $\mathbf{z}$ and $\mathbf{y}$ is

$$\mathbf{z}(t) = \mathbf{y}(t) + \mathbf{n}(t) + \mathbf{g}$$

where $\mathbf{n}(t)$ represents errors with zero bias, referred to as "noise" and $\mathbf{g}$ represents all bias errors. In summary, $\mathbf{x}$ is the model response, $\mathbf{y}$ is the model observations, and $\mathbf{z}$ is the actual measurement.

The objective is to minimize the difference between $\mathbf{z}(t)$ and $\mathbf{y}(t)$ in some sense, so that an appropriate cost functional is

$$J = \int_0^T \left[\mathbf{z}(t) - \mathbf{y}(t)\right]^T D_1 \left[\mathbf{z}(t) - \mathbf{y}(t)\right] dt$$

where D_1 is a weighting matrix reflecting the relative confidence in the measurements (similar to the inverse of the covariance of noise). Now that the cost functional has been completely specified, the only remaining step in the systems identification problem is to choose an algorithm for minimizing this cost functional.

Gradient Method

Probably the simplest minimization technique is the gradient technique, which changes the coefficients to be estimated by proceeding in the direction of the greatest decrease of the cost functional. Notationally, it is convenient to define a column vector, $\mathbf{c}$, of the unknowns to be estimated. The elements of $\mathbf{c}$ are some or all of the unknown elements of A and B (hence, G and H) of the initial conditions $\mathbf{x}(0)$ and of the noise biases $\mathbf{g}$, that is,

$$\mathbf{c} = \mathbf{c}\left[a_{ij},\ b_{ij},\ g_i,\ x_i(0)\right]$$

The gradient of J with respect to the vector $\mathbf{c}$ can be expressed in terms of the gradient of $(\mathbf{z} - \mathbf{y})$ as

$$\nabla_{\mathbf{c}} J = 2\left\{\int_0^T (\mathbf{z} - \mathbf{y})^T D_1 \nabla_{\mathbf{c}} (\mathbf{z} - \mathbf{y})\right\}^T dt \tag{7}$$

Thus, all that is needed to specify $\nabla_{\mathbf{c}} J$ in addition to terms already defined is $\nabla_{\mathbf{c}} (\mathbf{z} - \mathbf{y})$, as follows:

$$\nabla_{\mathbf{c}} (\mathbf{z} - \mathbf{y}) = -\left\{\nabla_{\mathbf{c}}\begin{bmatrix} I \\ \overline{G} \end{bmatrix}\right\}\mathbf{x} - \begin{bmatrix} I \\ \overline{G} \end{bmatrix}\nabla_{\mathbf{c}}\mathbf{x} - \left\{\nabla_{\mathbf{c}}\begin{bmatrix} I \\ \overline{H} \end{bmatrix}\right\}\mathbf{u} - \begin{bmatrix} I \\ \overline{H} \end{bmatrix}\nabla_{\mathbf{c}}\mathbf{u} - \begin{bmatrix} I \\ \overline{G} \end{bmatrix}\nabla_{\mathbf{g}}(\mathbf{z} - \mathbf{y}) \tag{8}$$

The gradient of $\mathbf{z}$ is affected only by the bias terms. The quantity $\nabla_{\mathbf{c}} (\mathbf{z} - \mathbf{y})$ can be expressed in terms of various partial derivatives. These partial derivatives with respect to the individual coefficients of $\mathbf{c}\,(a_{ij},\ b_{ij},\ g_i,\ x_i(0))$ are

$$\frac{\partial\begin{bmatrix} I \\ \overline{G} \end{bmatrix}}{\partial a_{ij}}\mathbf{x} = \begin{bmatrix} 0 \\ 0 \\ \vdots \\ x_j \\ \vdots \\ 0 \end{bmatrix}$$

$$\frac{\partial\begin{bmatrix} I \\ \overline{G} \end{bmatrix}}{\partial b_{ij}}\mathbf{x} = \begin{bmatrix} 0 \\ 0 \\ \vdots \\ 0 \end{bmatrix} \qquad \frac{\partial\begin{bmatrix} I \\ \overline{G} \end{bmatrix}}{\partial g_i}\mathbf{x} = \begin{bmatrix} 0 \\ 0 \\ \vdots \\ 0 \end{bmatrix}$$

where x_j appears in the $i + P$ row of the vector

$$\frac{\partial\begin{bmatrix} I \\ \overline{H} \end{bmatrix}}{\partial a_{ij}}\mathbf{u} = \begin{bmatrix} 0 \\ 0 \\ \vdots \\ 0 \end{bmatrix} \qquad \frac{\partial\begin{bmatrix} I \\ \overline{G} \end{bmatrix}}{\partial x_i(0)}\mathbf{x} = \begin{bmatrix} 0 \\ 0 \\ \vdots \\ 0 \end{bmatrix}$$

$$\frac{\partial \begin{bmatrix} I \\ \hline H \end{bmatrix}}{\partial b_{ij}} \mathbf{u} = \begin{bmatrix} 0 \\ 0 \\ \vdots \\ u_j \\ \vdots \\ 0 \end{bmatrix}$$

$$\frac{\partial \begin{bmatrix} I \\ \hline H \end{bmatrix}}{\partial g_i(0)} \mathbf{u} = \begin{bmatrix} 0 \\ 0 \\ \vdots \\ 0 \end{bmatrix} \qquad \frac{\partial \begin{bmatrix} I \\ \hline H \end{bmatrix}}{\partial x_i(0)} \mathbf{u} = \begin{bmatrix} 0 \\ 0 \\ \vdots \\ 0 \end{bmatrix}$$

where u_j appears in the $i + P$ row of the vector. Thus, only the gradient of $\mathbf{x}$ with respect to $\mathbf{c}$ and the gradients of $(\mathbf{z} - \mathbf{y})$ with respect to the bias terms $\mathbf{g}$ remain, where

$$\nabla_{\mathbf{c}} \mathbf{x} = \begin{bmatrix} \frac{\partial p}{\partial C_1} & \frac{\partial p}{\partial C_2} & - - - - & \frac{\partial p}{\partial C_m} \\ \frac{\partial r}{\partial C_1} & \frac{\partial r}{\partial C_2} & - - - - & \frac{\partial r}{\partial C_m} \\ \frac{\partial \beta}{\partial C_1} & \frac{\partial \beta}{\partial C_2} & - - - - & \frac{\partial \beta}{\partial C_m} \\ \frac{\partial \varphi}{\partial C_1} & \frac{\partial \varphi}{\partial C_2} & - - - - & \frac{\partial \varphi}{\partial C_m} \end{bmatrix}$$

A column is needed for each element of $\mathbf{c}$, which includes unknown elements in A and B, initial conditions, and bias terms.

The elements of the gradient $\mathbf{x}$ can be determined in the following manner. If the state equation is differentiated with respect to a_{ij}, for example,

$$\frac{\partial \dot{\mathbf{x}}}{\partial a_{ij}} = \frac{\partial A}{\partial a_{ij}} \mathbf{x} + A \frac{\partial \mathbf{x}}{\partial a_{ij}} + \cancelto{0}{\frac{\partial B}{\partial a_{ij}} \mathbf{u}} + B \cancelto{0}{\frac{\partial \mathbf{u}}{\partial a_{ij}}} \tag{9}$$

$$= A \frac{\partial \mathbf{x}}{\partial a_{ij}} + A_{a_{ij}} \mathbf{x}$$

The solution for $\frac{\partial x}{\partial a_{ij}}$ can be expressed as

$$\frac{\partial x}{\partial a_{ij}}(t) = \int_0^t e^{A(t-\tau)} A_{a_{ij}} x(\tau)\, d\tau$$

A similar procedure for coefficients in B gives the expression

$$\frac{\partial x}{\partial b_{ij}}(t) = \int_0^t e^{A(t-\tau)} B_{b_{ij}} u(\tau)\, d\tau$$

and, when used for elements of the initial conditions $x(0)$, results in

$$\frac{\partial x(t)}{\partial x_i(0)} = e^{At} \begin{bmatrix} 0 \\ \vdots \\ 1 \\ \vdots \\ 0 \end{bmatrix}$$

where the 1 appears in the i^{th} row. The corresponding partial derivatives with respect to constant bias errors in measuring the state variables can be expressed as follows:

$$\frac{\partial (z - y)}{\partial g_i} = \begin{bmatrix} 0 \\ \vdots \\ 0 \\ 1 \\ 0 \\ \vdots \\ 0 \end{bmatrix}$$

where the 1 appears in the i^{th} row.

Thus, all the terms in equation (8) have been defined; $\nabla_c J$ can now be evaluated by using equation (7). To obtain a gradient solution that minimizes J, the following recursive relation is used:

$$c_{k+1} = c_k - \epsilon \nabla_c J$$

where the subscript k is the index of the iteration. The value of ϵ can be chosen in many different ways. One way is to use 70 percent of the value that minimizes the fit error in one iteration. The gradient method was successful for only a few unknowns but failed otherwise. Theoretically, each iteration reduces the cost or fit error, but in practice the reductions become almost infinitesimal. Unfortunately, although the fit

error is reduced considerably before it stalls, the corresponding values of the unknown coefficients are not determined with sufficient accuracy, because the minimum is never reached.

Many methods have been developed for nonlinear minimization, such as direct-search techniques and accelerated gradient techniques (ref. 11), but for this particular application a modified Newton-Raphson technique was chosen.

Modified Newton-Raphson Minimization Technique

Minimization based only on flight data. - The Newton-Raphson technique is an iterative method for finding a zero of a nonlinear function of several parameters, or, in this instance, a zero of the gradient of the cost functional, that is,

$$\nabla_c J = 0$$

Consider a two-term Taylor's series expansion of $\nabla_c J$ about the k^{th} value of c_k:

$$(\nabla_c J)_{k+1} \approx (\nabla_c J)_k + \left(\nabla_c^2 J\right)_k \Delta c_{k+1} \tag{10}$$

with

$$\Delta c_{k+1} = (c_{k+1} - c_k)$$

where $\left(\nabla_c^2 J\right)_k$ is the second gradient of the cost functional with respect to c, or the Hessian matrix, at the k^{th} iteration. If equation (10) is a sufficiently close approximation, the change in c on the $(k + 1)$ iteration to make $(\nabla_c J)_{k+1}$ approximately zero is

$$\Delta c_k = - \left[\left(\nabla_c^2 J\right)_k\right]^{-1} (\nabla_c J)_k \tag{11}$$

which is the Newton-Raphson algorithm, as shown in the following sketch:

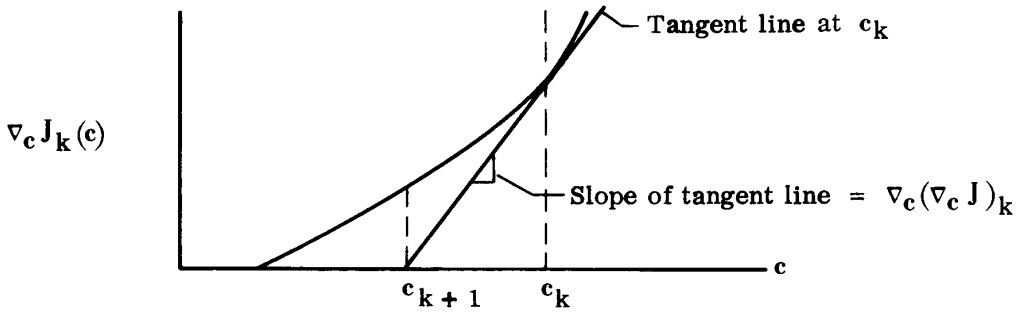

This method is much more efficient than the gradient method because it attempts to predict where the local minimum point is and to step directly to it rather than merely

stepping in the local downhill direction. However, it is much more complex because of the computation of the second gradient matrix. This complexity can be reduced significantly by an appropriate approximation to the second gradient matrix which results in a method termed either modified Newton-Raphson or quasi-linearization. It is most clearly derived by the method of quasi-linearization.

The difference between the measured and computed responses, $\mathbf{z}(t) - \mathbf{y}(t)$, can be represented as quasi-linear with respect to a change in the unknown coefficients, that is,

$$\left[\mathbf{z}(t) - \mathbf{y}(t)\right]_k \approx \left[\mathbf{z}(t) \quad \mathbf{y}(t)\right]_{k-1} + \nabla_c \left[\mathbf{z}(t) - \mathbf{y}(t)\right]_k \Delta \mathbf{c}_k \tag{12}$$

Using this approximation in the cost functional results in the following first and second gradients:

$$\nabla_c J = 2\left\{\int_0^T (\mathbf{z} - \mathbf{y})_k^T \; D_1 \left[\nabla_c (\mathbf{z} - \mathbf{y})\right]_k dt\right\}^T$$

$$\nabla_c^2 J = 2\int_0^T \left[\nabla_c (\mathbf{z} - \mathbf{y})\right]_k^T D_1 \left[\nabla_c (\mathbf{z} - \mathbf{y})\right]_k dt$$

Now the modified Newton-Raphson algorithm becomes

$$\Delta \mathbf{c}_k = -\left\{\int_0^T \left[\nabla_c (\mathbf{z} - \mathbf{y})\right]_k^T D_1 \left[\nabla_c (\mathbf{z} - \mathbf{y})\right]_k dt\right\}^{-1} \int_0^T \left[\nabla_c (\mathbf{z} - \mathbf{y})\right]_k^T D_1 (\mathbf{z} - \mathbf{y})_k \, dt \tag{13}$$

All the terms in equation (13) involve only the first gradients of $(\mathbf{z} - \mathbf{y})$, which were derived previously and are readily computed. Thus equation (13) involves no second gradients of $(\mathbf{z} - \mathbf{y})$ which would appear in the true $\left(\nabla_c^2 J\right)$. This greatly reduces the computation time, and the approximation improves as the solution is approached. All the preceding terms have been derived for the gradient techniques, so the solution is readily obtained.

Because the minimization by the Newton-Raphson technique is done in the discrete case by a digital computer, the discrete approximation transforms the integrals into summations. Equation (13) becomes

$$\Delta \mathbf{c} = \left\{\sum_{i=1}^{l} \left[\nabla_c (\mathbf{z}^i - \mathbf{y}^i)\right]^T D_1 \nabla_c \left(\mathbf{z}^i - \mathbf{y}^i\right)\right\}^{-1} \sum_{j=1}^{l} \left[\nabla_c \left(\mathbf{z}^j - \mathbf{y}^j\right)^T D_1 \left(\mathbf{z}^j - \mathbf{y}^j\right)\right] \tag{14}$$

where the superscripts i and j are the indices indicating the time sample, and l is the total number of samples.

Although the difference in notation might disguise the fact, the preceding solution is the same as that obtained with the Newton-Raphson method if the term involving the second gradient multiplied by the noise is neglected as suggested by Balakrishnan in reference 5. The savings in computation is considerable.

All subsequent references to the Newton-Raphson method will be based upon the modified Newton-Raphson approach to minimization of the integral-squared error.

To keep computer usage to a minimum, no noise biases or initial conditions were determined for the X-15 data used, thus

$$c^T = \left(L_p \quad L_r \quad L_\beta \quad L_{\delta_a} \quad L_{\delta_r} \quad L_{\delta_0} \quad N_p \quad N_r \quad N_\beta \quad N_{\delta_r} \quad N_{\delta_a} \quad N_{\delta_0} \quad Y_p \quad Y_\beta \quad Y_{\delta_0} \right)$$

Figure 9 shows the rapid reduction in the weighted fit error, J, when the Newton-Raphson method is used. For the example shown, only four iterations were necessary. This represents a computation time of about 7 minutes on the XDS 9300 digital computer (ref. 12). The Newton-Raphson method has been found to be superior to the gradient method both in terms of the number of iterations and the computation time required for the application under discussion.

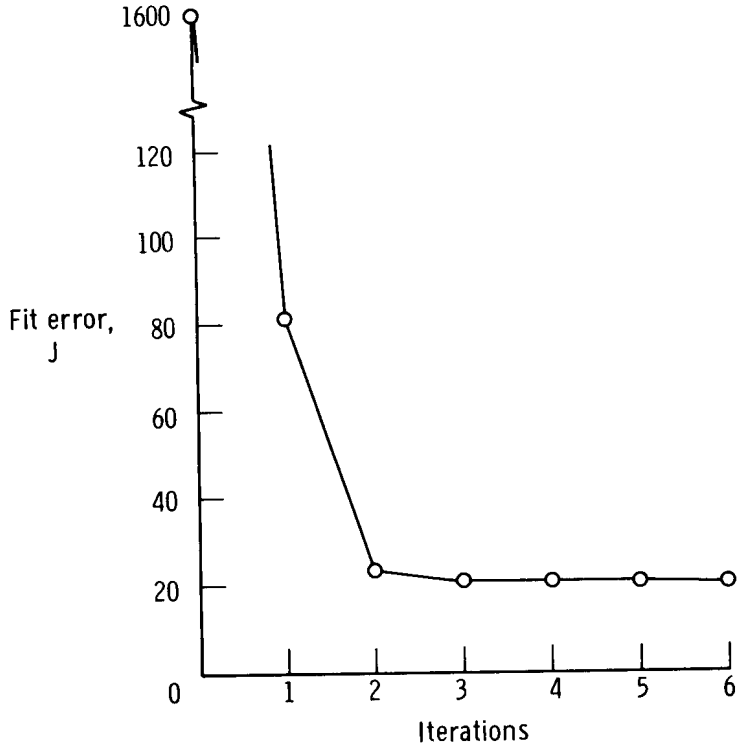

Figure 9. Convergence of fit error for the modified Newton-Raphson method.

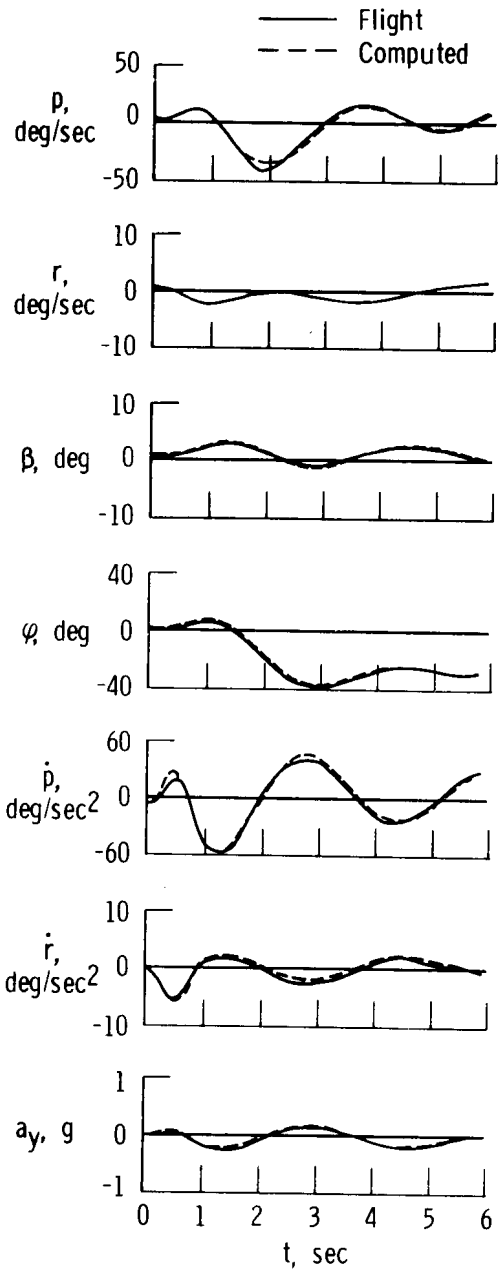

Figure 10. Comparison of X-15 time histories measured in flight and computed by using coefficients obtained from flight data with the modified Newton-Raphson method.

Figure 10 shows the computed state time histories compared with the measured time histories. The corresponding weighted mean-square-fit error is 0.2 percent of that obtained with the least-squares method. Most of the reduction is attributed to the improved fit of φ. The fits of p and r are also improved, as expected, because the cost functional was chosen on the basis of optimizing with respect to the integral squared error of the difference between measured and computed data.

Minimization including a priori information. - Often, independent estimates of the values of the coefficients are available from wind-tunnel data or previously obtained flight data. It is desirable to incorporate this a priori information into the flight data. The use of the a priori values in the Newton-Raphson method resembles the procedure often followed in analog matching in which, initially, the predictions based upon wind-tunnel values are used and changes made to improve the fit are weighted against the departure from these values. It seems reasonable then to use the a priori feature with the Newton-Raphson method, making use of all the information available to obtain the estimates and insuring that no change is made in the derivatives unless there is sufficient information in the flight data. The procedure used is to expand the cost expression to include a penalty for departure from the a priori values. The expanded cost becomes

$$J = \int_0^T (z - y)^T D_1 (z - y)\, dt + (c - c_0)^T K D_2 (c - c_0) \tag{15}$$

where c_0 is the vector of a priori estimates of c.

Recognizing the solution obtained by using Newton-Raphson to be of the form

$$\Delta c = - \left[\nabla_c^2 J\right]^{-1} \nabla_c J$$

and the contributions to the first and second gradients due to the additional term to the cost expression to be $D_2 (c - c_0)$ and D_2, respectively, the new expressions become

$$\nabla_c J = 2\left\{\int_0^T (z-y)^T D_1 \left[\nabla_c (z-y)\right] dt\right\}^T + 2\,K\,D_2 (c - c_0)$$

$$\nabla_c^2 J = 2\int_0^T \left[\nabla_c (z-y)\right]^T D_1 \nabla_c (z-y)\, dt + 2\,K\,D_2$$

If the a priori information is based upon previously analyzed flight data, the selection of the D_2 matrix can be based upon the relative amounts of data involved and the expected variance of c_0. If the a priori values are obtained from wind-tunnel tests, it becomes necessary to estimate the variance of these values, as discussed in the next section.

Figure 11 is an example of how the fit error changes as the weighting of the a priori values is changed. The weighting was varied by changing the weighting factor, K (a scalar), multiplied by D_2. For a weighting of zero the a priori values are ignored, and for an infinite weighting the flight data are ignored. Shown in the same figure are two

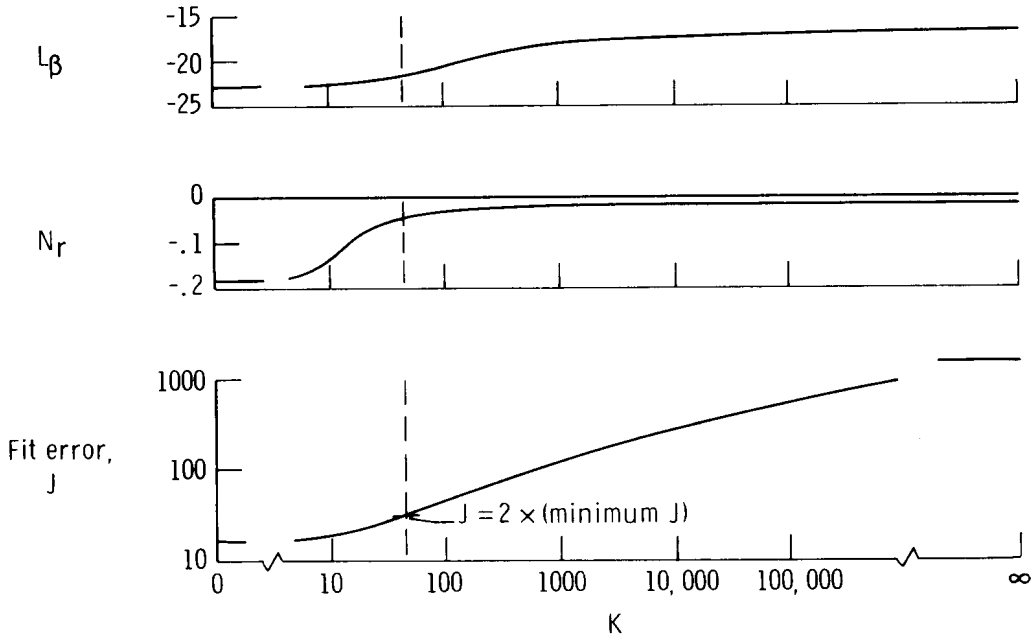

Figure 11. Effect of a priori weighting on coefficients and the fit error.

coefficients as a function of the same weighting factor. It is noteworthy that the coefficient N_r changes immediately to its a priori value, but the coefficient L_β does not. It would appear that the estimate of the coefficient N_r is weaker in the sense that it could vary over a wide range with little effect on the fit error.

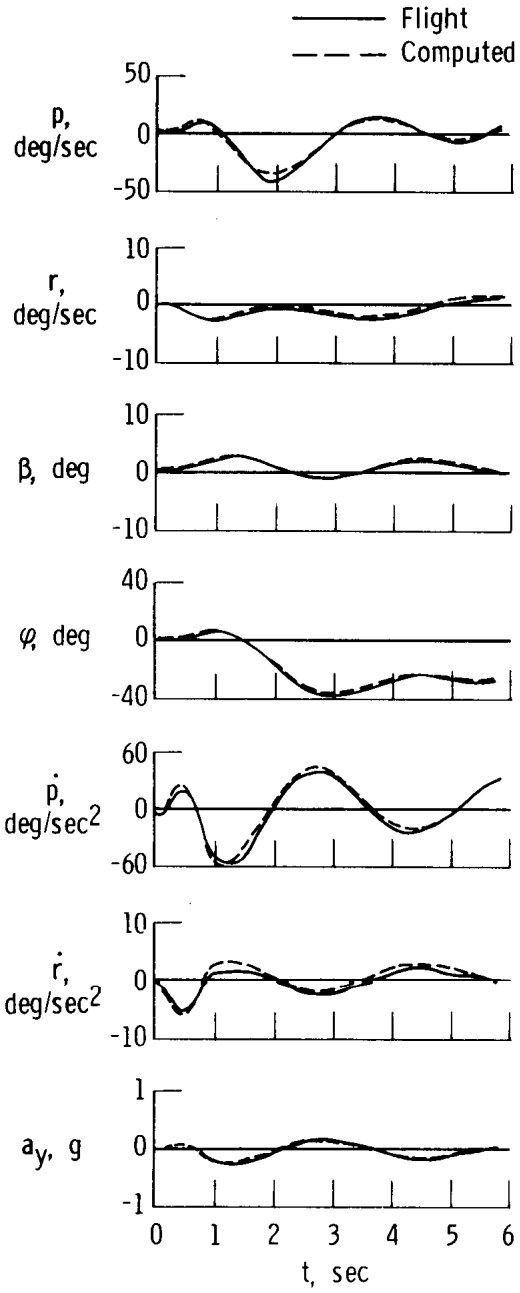

Figure 12. Comparison of the X-15 time histories measured in flight and computed by using coefficients obtained from flight data with the modified Newton-Raphson method with an a priori weighting which doubles the unweighted fit error.

A weighting factor was used that doubled the fit error. Although the fit error is necessarily increased when a priori information is used, figure 12 shows that the agreement of the computed and measured time histories is still good. The use of a priori information in estimating the unknowns has been found to reduce the scatter of the estimates (especially when the flight data contain little information on a given coefficient) and to reduce the number of iterations to convergence. However, more computer time may be required in selecting the overall gain, K, of the a priori weighting.

Weighting Matrices

Since the cost functional in equation (15) contains the weighting matrices, D_1 and D_2, it should be expected that these matrices play major roles in the value obtained for each of the coefficients. There are many ways of determining the D_1 and D_2 weighting matrices; the following discussion describes the method found to be most useful in this study.

A reasonable selection of the weighting matrix, D_1, can be based upon knowledge of the statistical properties of the instrumentation noise. If the noise were stationary, Gaussian, and white,

$$d_{1_{ii}} = \frac{1}{E\left\{n_i^2\right\}}$$

would be the obvious weighting for mean-square minimization. In practice the best fit "obtainable" for a particular quantity was used as an indication of its noise level, in the following manner. An estimate of the noise was made for each variable, and the matrix was assumed to be diagonal. As more experience was acquired through using the data, the diagonal elements were changed if a particular fit of a given variable produced an average error smaller than the original estimate. The new value of the element would be the reciprocal of the new minimum integral error squared in the measurement of that variable. Gradually, a new D_1 matrix based on the minimum

average error evolved, and further changes were unnecessary.

It should be stressed that much more research is needed in determining a representative nondiagonal D_1 weighting matrix. This can be done adequately only by completely analyzing the instrumentation used to obtain these measurements. Primarily, such an investigation would supply a covariance matrix of the noise in the output of a given instrumentation system. In addition, such information as phase shift, amplitude attenuation, and nonlinearities of the instrumentation dynamics, both electrical and mechanical, is critical to any analysis of the data. The more representative the data are of the true observation **y**, the more satisfactory the results by any method of estimation. The elements of the D_1 matrix can readily be determined along with the other unknowns; although the instrumentation remains the same, a different noise covariance matrix will result for each maneuver.

The values used for D_1 are listed in table 1. If part of the data is unusable, the corresponding element of D_1 should be set to zero. This procedure offers an advantage over other methods, such as the least squares or Shinbrot, which require a complete set of data. The integral-squared-error method can determine all unknowns, even when the data used are incomplete.

TABLE 1.–VALUES USED IN THE D_1 AND D_2 WEIGHTING MATRICES FOR THE X-15 AIRPLANE

i	d_{1ii}	y_i	d_{2ii}	c_i
1	1,530	p	0.1445	$L_{\delta a}$
2	1,040,000	r	.1445	$L_{\delta r}$
3	507,000	β	0	$L_{\delta 0}$
4	31,700	φ	522	L_p
5	635	$\dot{p}$	5.22	L_r
6	46,800	$\dot{r}$	.1445	L_β
7	5.333	a_y	14.45	$N_{\delta a}$
8	------	-	14.45	$N_{\delta r}$
9	------	-	0	$N_{\delta 0}$
10	------	-	815.5	N_p
11	------	-	815.5	N_r
12	------	-	14.45	N_β
13	------	-	0	$Y_{\delta 0}$
14	------	-	13,010	Y_p
15	------	-	13,010	Y_β

The D_2 matrix for weighting wind-tunnel estimates would ideally be the inverse of

the error covariance matrix of the test data from which the estimates were obtained, inasmuch as this would reflect the relative confidence in each of the a priori values. Since the covariance matrix was not available, the following method, which is only one of many justifiable procedures, was used to obtain the D_2 matrix. No attempt will be made to show that this method is preferable to other methods. The estimates are assumed to be independent, which results in D_2 being a diagonal matrix. Next, on the basis of experience with wind-tunnel estimates, a wind-tunnel variance, σ_{ii}^2, was selected for each of the unknown coefficients. An attempt was made to use the same variance for similar coefficients (L_{δ_a}, L_{δ_r}, and L_β, because they are determined in a similar manner in the wind tunnel). Now D_2 was determined by taking the reciprocal of each variance, $\frac{1}{\sigma_{ii}^2}$ and inserting it as the appropriate element along the diagonal of D_2. (These values are shown in table 1.) This fixed the relative weighting among the individual coefficients. The overall weighting of the wind-tunnel coefficients to the flight-data-determined coefficients was changed by varying the values of K.

Comparison of Methods

From a comparison of the time histories shown previously, it is evident that the Newton-Raphson method without the a priori feature provides the best fit of computed data with the flight time history, and there is only a slight change in the quality of the fit with the addition of the a priori feature. In addition to the time history fit, it is also of interest to compare the stability derivatives obtained with the various methods. These stability derivatives are shown in figure 13 together with derivatives predicted from wind-tunnel data. Because of the uncertainties in the wind-tunnel predictions as well as in the flight-determined coefficients, the only definite conclusions that can be reached regarding the superiority of any of the methods is that the Newton-Raphson method with the a priori feature provides the closest match of both the flight data and the a priori values. When the derivatives determined by the Newton-Raphson method with and without the a priori feature have approximately the same values, it can be concluded that these are the strong, well-defined derivatives. Thus L_β and L_{δ_a} are strong derivatives. For N_r and N_{δ_a} there is a large difference between the Newton-Raphson method with and without the a priori feature, which indicates a weakly defined derivative; similarly, the results from the other methods show little agreement with one another. In this instance there is not sufficient information in the flight data to strongly define N_r, and the wind-tunnel estimate is as good as any other estimate.

To make a more rigorous comparison, a statistical model was constructed and used to indicate the relative values of variance in the estimates obtained by using the least-squares, Shinbrot, and Newton-Raphson methods. Specifically, a time history was computed, and actual measured flight data were simulated by adding shaped, unbiased white noise. The noise was approximated as the error, $\mathbf{n}(t)$, for a best fit "obtainable" for each quantity in the actual flight data previously analyzed. The power spectral densities were determined for each quantity; however, they were approximately the same, so only one statistical representation of the noise was used for all the quantities. Five time histories were generated which differed only in the specific noise added and

were analyzed by each of the methods. Estimates of the variance and average value for each coefficient are shown in figure 14, in which the Newton-Raphson method provides

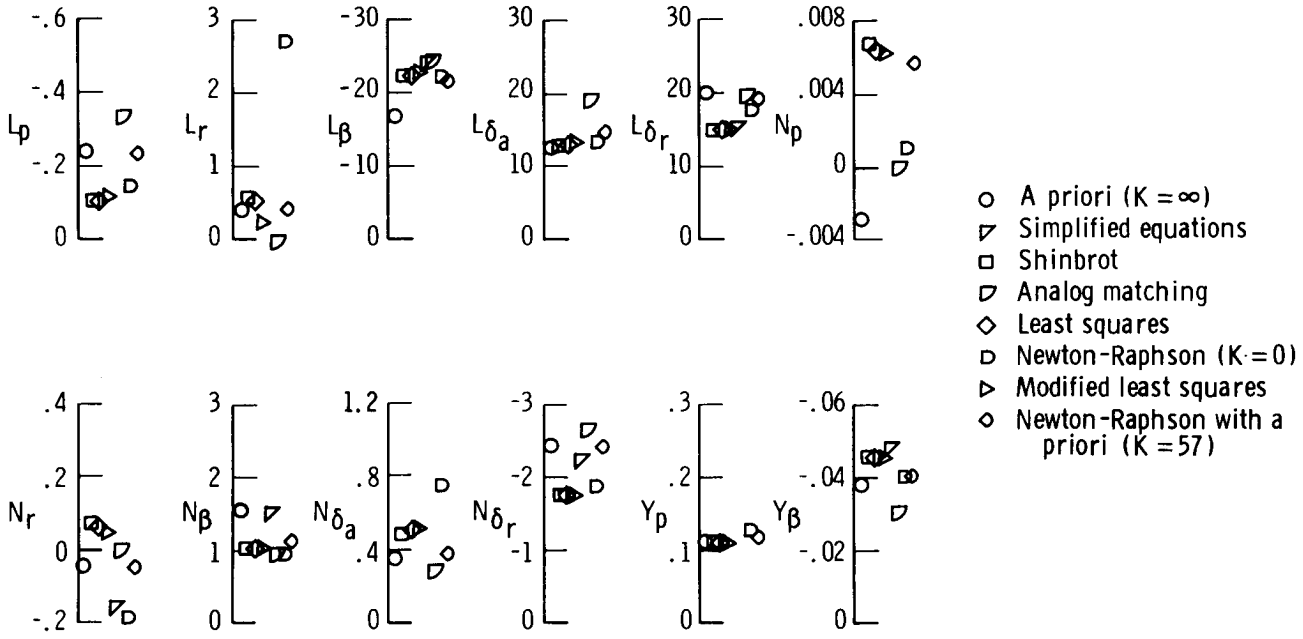

Figure 13. Comparison of coefficients determined from X-15 flight data by using several methods of analysis and predictions based upon wind-tunnel tests.

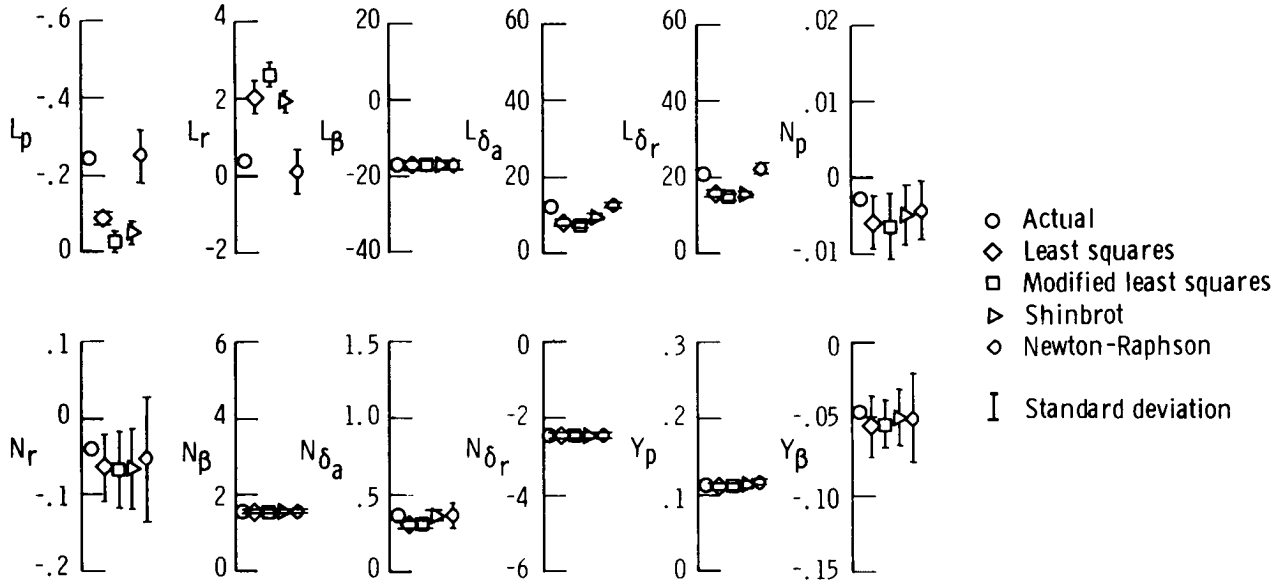

Figure 14. Comparison of results of applying several methods of analysis to computed time histories to which noise has been added.

the value closest to the actual value for every coefficient. Although the variance for the Newton-Raphson method is generally larger than that for the least-squares and Shinbrot methods, all the actual values are included within the $\pm 1\sigma_E$ band about the mean.

Cramèr-Rao Bound

It is of considerable interest in parameter estimation to assess the validity of the estimates of the unknown parameters. If the actual covariance matrix of the estimated parameters were known, it would indicate which parameters had been most reliably estimated. The error matrix of the estimates can be defined as

$$\Phi = E\left\{\left(\mathbf{c} - \mathbf{c}_T\right)\left(\mathbf{c} - \mathbf{c}_T\right)^T\right\}$$

where $\mathbf{c}$ is the current estimate and $\mathbf{c}_T$ is the "true" value of the parameter. The derivation in the appendix shows that this error matrix can be bounded from below by the matrix Cramèr-Rao bound (ref. 5). In other words, the bound provides the minimum variance with which any of the parameters may be estimated for a given set of data. It is on this basis that an approximation of the Cramèr-Rao bound is used in conjunction with the Newton-Raphson estimation to assess the amount of confidence to be placed in the various parameters estimated.

More specifically, by assuming that the estimates obtained by the Newton-Raphson method are asymptotically unbiased and the noise is a stationary Gaussian white noise process, a useful form of this bound may be obtained for a direct comparison with the results of the Newton-Raphson method. These assumptions simplify the expression for the matrix bound to

$$\Phi \geq \left\{\sum_{i=1}^{l} \nabla_{\mathbf{c}}\left[\mathbf{y}^i\right]^T D_1 \nabla_{\mathbf{c}}\left[\mathbf{y}^i\right]\right\}^{-1} \tag{16}$$

This expression is derived in the appendix. Although the specific data being analyzed do not conform exactly with the preceding assumptions, a comparison of this bound with the variance determined from the statistical model of the last section would give some insight into the relative reliability of the estimates. The assumption of asymptotically unbiased estimates can be shown to be reasonable because, through use of the Newton-Raphson method, the first term of equation (14) changes only slightly from one iteration to another. If no change occurs, this term can be deemed to be independent of the noise. Thus, if $\frac{\partial(\mathbf{z} - \mathbf{y})}{\partial g_i} = 0$, the noise is unbiased and $\Delta\mathbf{c}$ is a linear transformation of the noise. So, if the noise is unbiased, the estimate of the coefficient is unbiased. The assumption of the statistics of the noise is not met by the data, but the actual noise may be such that the Cramèr-Rao bound will give additional insight into the validity of the estimates obtained.

Because the first term in equation (14) is identical to the term derived for the Cramèr-Rao bound determined under the somewhat idealized assumptions, the approximation of the Cramèr-Rao bound is available in the computation of the Newton-Raphson

minimization. Figure 15 compares the standard deviations obtained by using the Cramèr-Rao bound from the Newton-Raphson computation with those obtained by analyzing the statistical model discussed in the preceding section and shown in figure 14. It

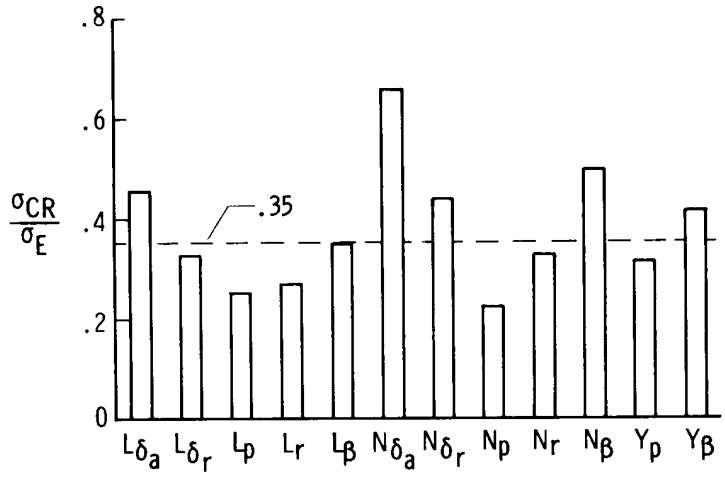

Figure 15. Comparison of the standard deviation indicated by the approximation of the Cramèr-Rao bound and by experiment.

should be noted that figure 15 shows that the standard deviation of the experimental model is greater than that predicted by the application of the Cramèr-Rao bound. The ratios of $\frac{\sigma_{CR}}{\sigma_E}$ are fairly well centered about 0.35. Thus, the theoretical result provides insight into the relative confidence that might be placed on the estimates.

If the coefficients of the a priori feature are to be used, it might be anticipated that the same computation may not represent an estimate of the Cramèr-Rao bound. However, the same type of information may be obtained with the a priori weighting by interpreting the calculation in the following way: If the total probability $\rho(\mathbf{z}, \mathbf{c}_T)$ were used instead of $\rho(\mathbf{z}|\mathbf{c}_T)$ in the derivation in the appendix, an expression similar to that for the Cramèr-Rao bound would be readily found. The cost functional associated with using the total probability is that used with the a priori feature.

The estimates without a priori information can be considered to have the D_2 matrix equal to the null matrix. The Cramèr-Rao bounds of the variances obtained are used to assess the reliability of the estimates of the coefficients. That is, if the variance is large, less confidence is placed in that estimate. In this instance, the variances obtained are compared with the inverse of the D_2 matrix, which is infinite for all coefficients. Therefore, the larger ("closer to infinity") the bound, the less confidence is placed in that estimate.

Generalizing to the case where D_2 is a nonsingular matrix, once again the bound of the variance should be compared with the inverse of D_2. So the computation

analogous to the Cramèr-Rao bound $[\sigma_{a_{ii}}]$ will satisfy $D_2^{-1} \geq \left[\sigma^2_{a_{ii}}\right]$. To make proper use of this information, the values of the bounds closer to the corresponding element of D_2^{-1} will correspond to the least reliable estimates. In the limiting case, the values would be identical. This would indicate that no additional information is contained in the data. Although the comparison is not made as readily for a non-null D_2 as for a null D_2, the information is still contained in the same computation. The result would not properly be called the Cramèr-Rao bound, but the relative reliability of the estimates can still be ascertained.

RESULTS FOR THREE CLASSES OF AIRCRAFT

The Newton-Raphson technique of minimizing the integral-squared error was applied to aircraft of widely varied geometry and flight regions to demonstrate the versatility of the method. A light general aviation airplane, a large supersonic airplane, and a lifting body vehicle were selected, in addition to the X-15 airplane discussed previously, to represent the extremes of modern aircraft. In all the vehicles a variable bias in measurement was allowed for the first three elements of the state vector (p, r, β). Variable bias was not used on the remaining measurements, nor were any variable initial conditions used, because the increased accuracy realized from these additional variables did not justify the computer time needed to solve for more unknowns. Not all the measurements available on the X-15 airplane were obtainable on every other vehicle. Two separate time histories were analyzed simultaneously on the XB-70 airplane to demonstrate how several time histories at the same flight condition may be analyzed together.

The D_1 (table 2) weighting matrices were generated in the manner discussed earlier. However, the D_2 weighting matrix was the same as that used previously, and only the overall scalar weighting, K, was changed for each vehicle. The overall weighting used was that which doubled the mean square error attained with zero weighting. As in the X-15 data previously analyzed, the a priori values used were the predicted values based upon wind-tunnel tests.

Light General Aviation Airplane

To show that the method can be applied to a low-speed, light, conventional airplane, a rudder maneuver for a light twin-engine (ref. 13) airplane was chosen. In figure 16 a flight time history of this airplane is compared with a time history computed from the a priori values based primarily on wind-tunnel data. It should be noted that bank angle, φ, was not measured and no aileron input was made. Thus, the aileron derivatives were not determined, but the match was still attempted. To obtain the match, the element of D_1 corresponding to φ was set to zero.

In figure 17 the measured data are compared with the Newton-Raphson solution with no a priori weighting. It is obvious that the Newton-Raphson solution more closely approximates the flight data than do the wind-tunnel estimates. The most significant

TABLE 2.–VALUES USED FOR THE D_1 WEIGHTING MATRICES FOR A LIGHT AIRPLANE, THE XB-70 AIRPLANE, AND A LIFTING BODY VEHICLE

		Light airplane	XB-70	Lifting body
Lateral - Directional				
i	y_i	$d_{1_{ii}}$	$d_{1_{ii}}$	$d_{1_{ii}}$
1	p	103,000	13,400	14,300
2	r	33,300	562,000	353,000
3	β	294,000	208,000	289,000
4	φ	0	75,500	9,900
5	$\dot{p}$	25,300	0	0
6	$\dot{r}$	57,100	0	0
7	a_y	13,100	27,700	24,000
Longitudinal				
i	y_i	- - - - -	$d_{1_{ii}}$	- - - - -
1	q	- - - - -	20,000	- - - - -
2	α	- - - - -	3,431	- - - - -
3	V	- - - - -	0	- - - - -
4	Θ	- - - - -	0	- - - - -
5	$\dot{q}$	- - - - -	800	- - - - -
6	a_z	- - - - -	200	- - - - -
7	a_x	- - - - -	0	- - - - -

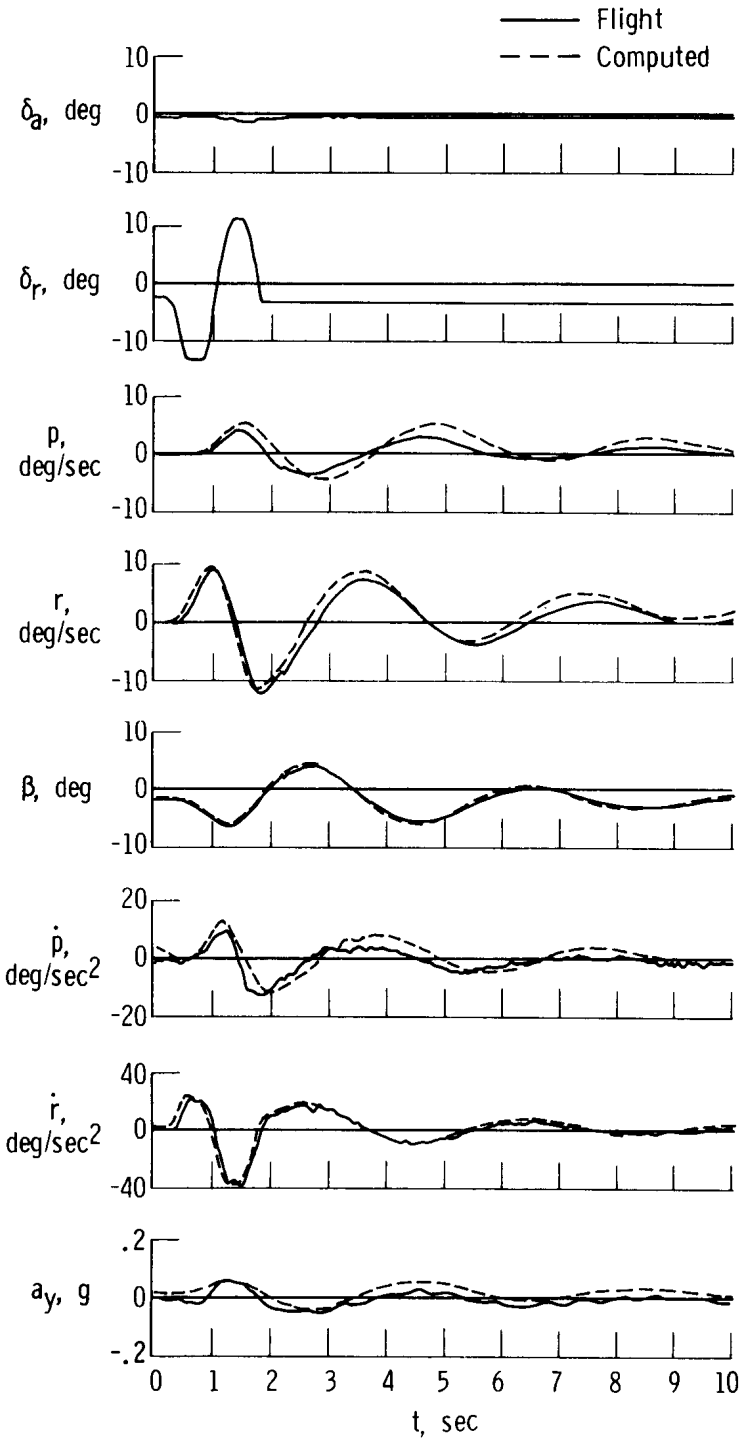

Figure 16. Comparison of light airplane time histories measured in flight and computed by using a priori values. K = ∞.

departure is in the a_y trace.

Figure 18 compares the flight data with the time history computed by using the Newton-Raphson method with an overall a priori weighting of K = 1.0. The fit is improved somewhat over that in figure 17 in some of the signals but is poorer in others, including a_y.

Figure 19 is a summary of the coefficients obtained by the three different methods. It should be noted that the coefficients used for the a priori values of L_p, L_r, N_p, and N_r were computed from the vehicle geometry and other aerodynamic characteristics and not obtained from wind-tunnel data. The wind-tunnel fit and the a priori weighted fit agree fairly well except for L_β, L_r, and Y_β. The coefficient L_β is particularly interesting, in that it was forced away from the a priori value in order to improve the correlation with the other coefficients. It appears that there is a significant amount of information in the flight data to indicate that Y_β should not actually be at the a priori value. Also, it is interesting to note that L_p, N_p, and N_{δ_r} are at the a priori value when weighted and show a significant departure when unweighted. This supports the conclusion that little information on these coefficients is contained in the data. Although this might be attributed to the relative weighting in the D_2 matrix, which certainly is a primary factor, L_β and N_p exhibited the opposite behavior for the X-15 airplane

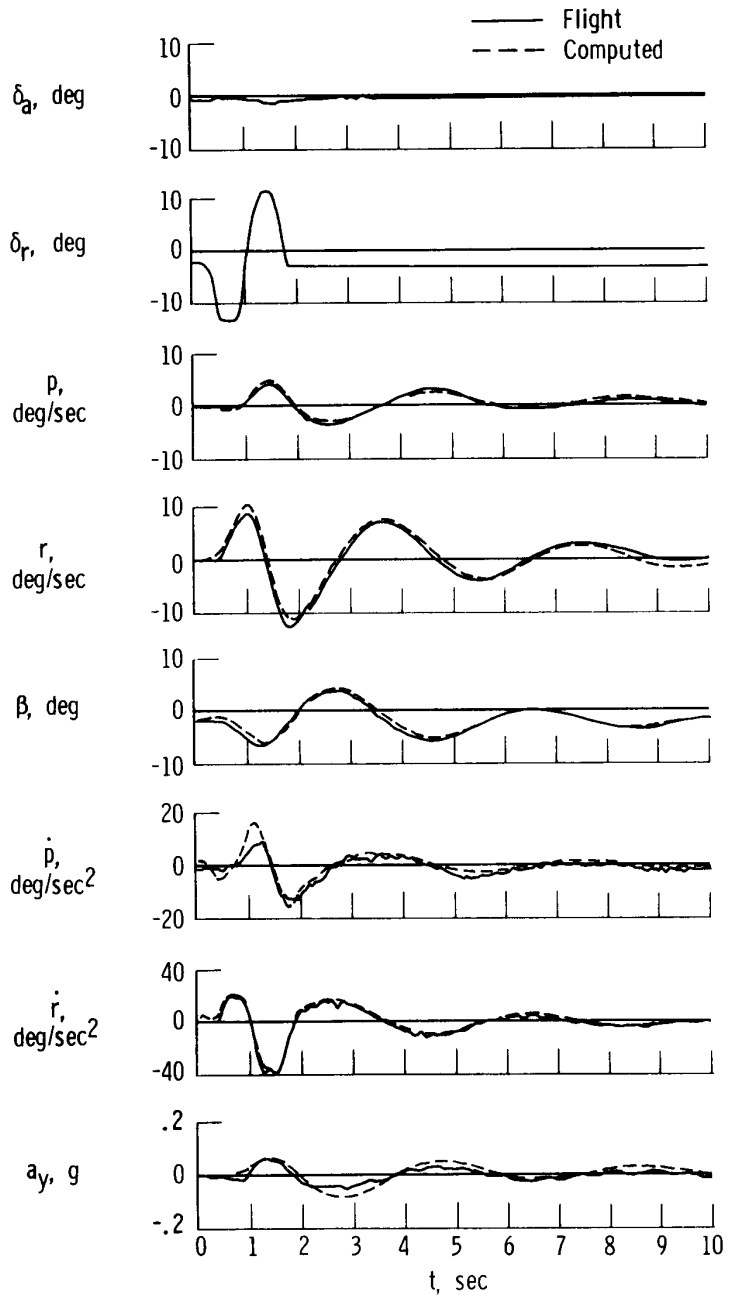

Figure 17. Comparison of light airplane time histories measured in flight and computed by using coefficients obtained from flight data with the modified Newton-Raphson method without a priori weighting. K = 0.

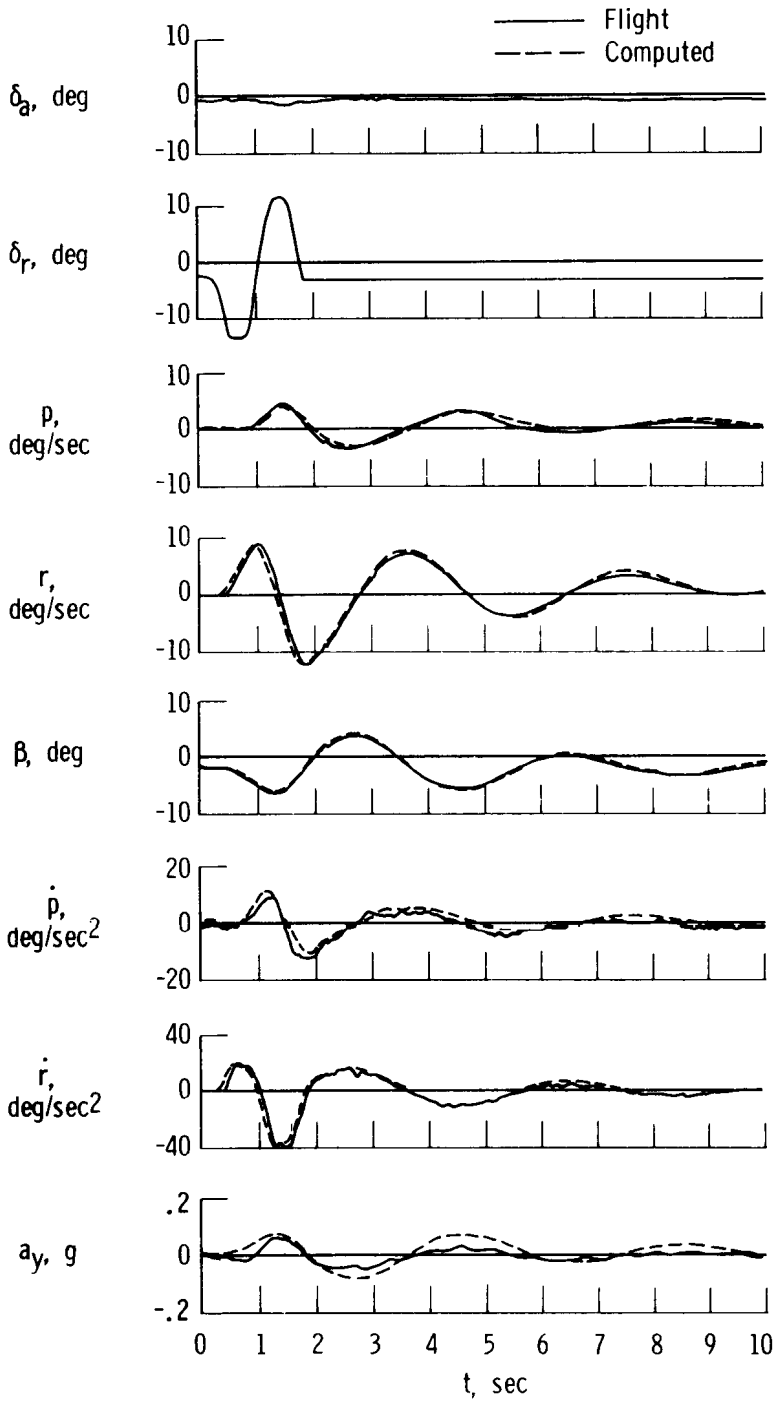

Figure 18. Comparison of light airplane time histories measured in flight and computed by using coefficients obtained from flight data with the modified Newton-Raphson method with an a priori weighting which doubles the unweighted fit error. K = 1.0.

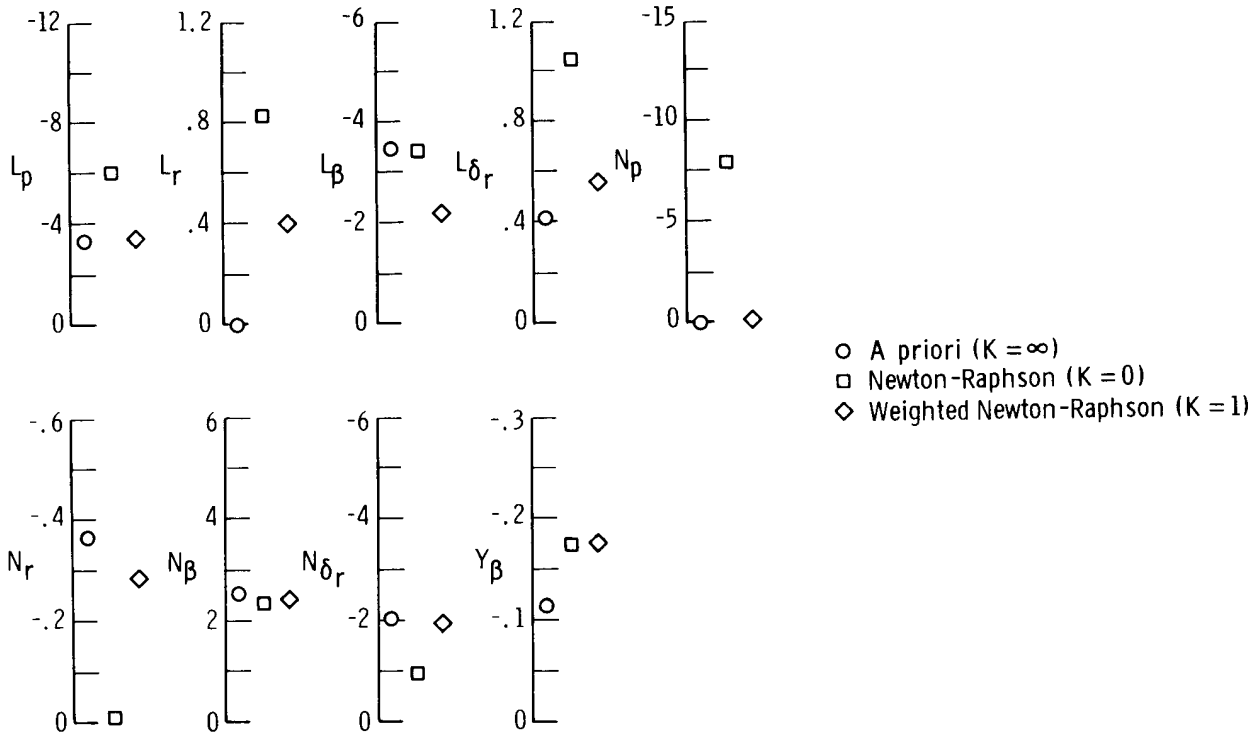

Figure 19. Comparison of light airplane coefficients determined from flight data by using a modified Newton-Raphson method and from a priori estimates.

data which had the same relative weighting. This points up once again the need for more information on the covariance matrix of the wind-tunnel data which are intuitively the values desired for the D_2 matrix. Of course, the covariance matrix of wind-tunnel estimates would be different for each vehicle.

Large Supersonic Airplane

The large, supersonic-cruise XB-70 airplane (ref. 14) was chosen to represent this extreme in aircraft. The maneuvers selected consisted of an aileron, δ_a, maneuver followed by a rudder, δ_r, maneuver at a later time in the same flight at essentially the same flight condition. The two maneuvers were analyzed simultaneously. Figures 20(a) and 20(b) compare the flight time histories of the two maneuvers with the computed time histories based upon wind-tunnel estimates modified for elasticity effects (a priori). The $\dot{p}$ and $\dot{r}$ signals were not measured, but the match was obtained by setting the corresponding elements of D_1 equal to zero (table 2). In contrast to the fit for the light airplane, the agreement is poor. There is considerable drift in all the signals largely because of the unknown bias in the controls, except φ and r, and the amplitudes are vastly different on the p and β signals..

The ability to match both time histories simultaneously would be a distinct advantage over some of the current methods of obtaining coefficients. With these techniques the control derivatives L_{δ_r}, N_{δ_r}, and Y_{δ_r} could not be determined from the time

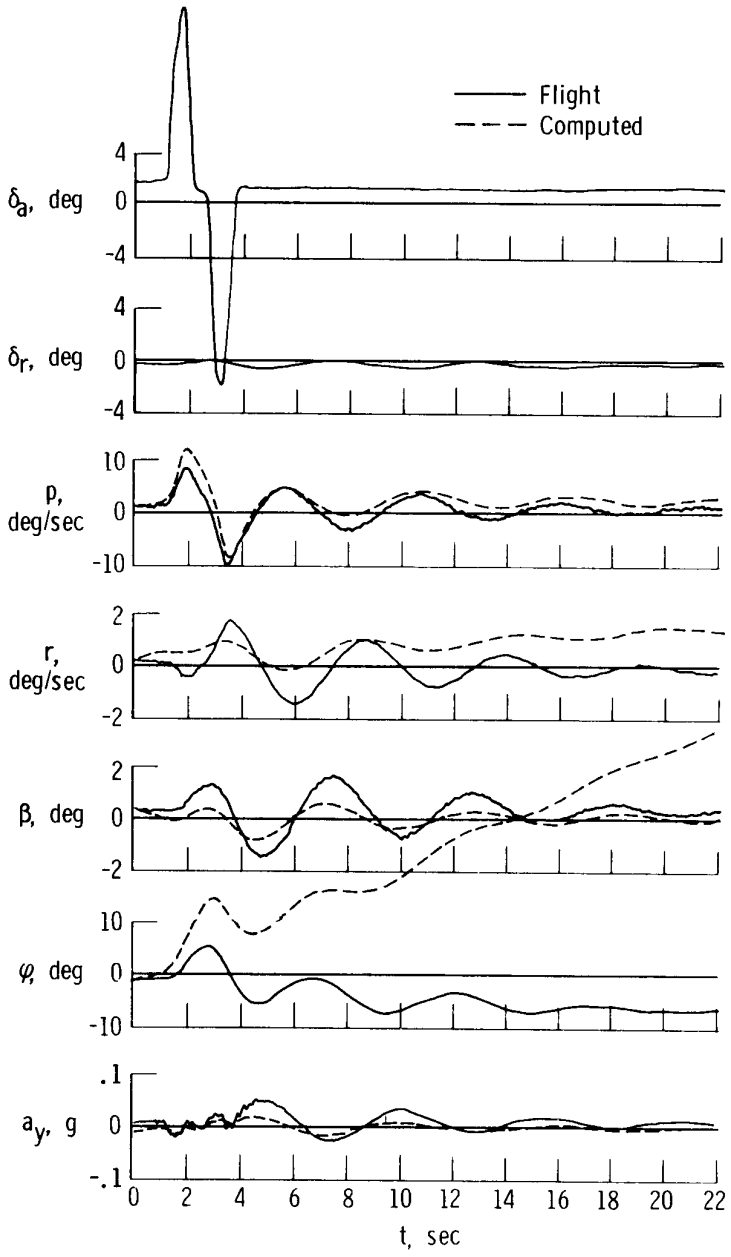

(a) First maneuver.

Figure 20. Comparison of the XB-70 time histories measured in flight and computed by using a priori values. $K = \infty$.

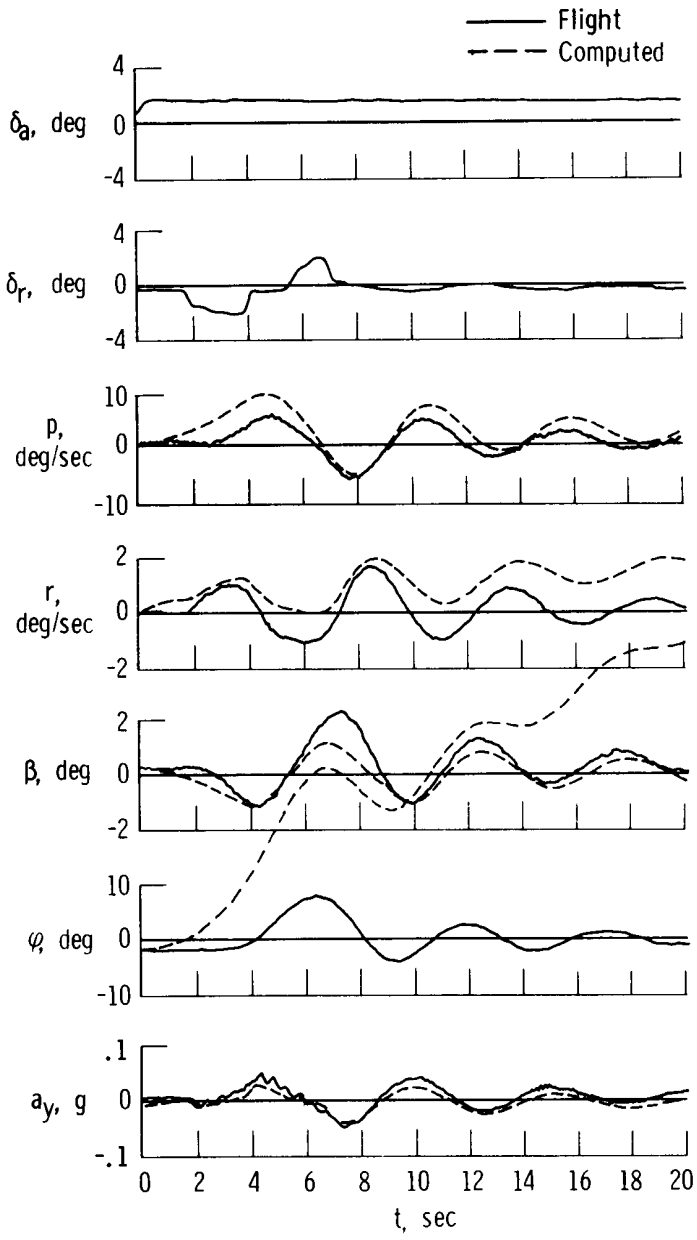

(b) Second maneuver.

Figure 20. Concluded.

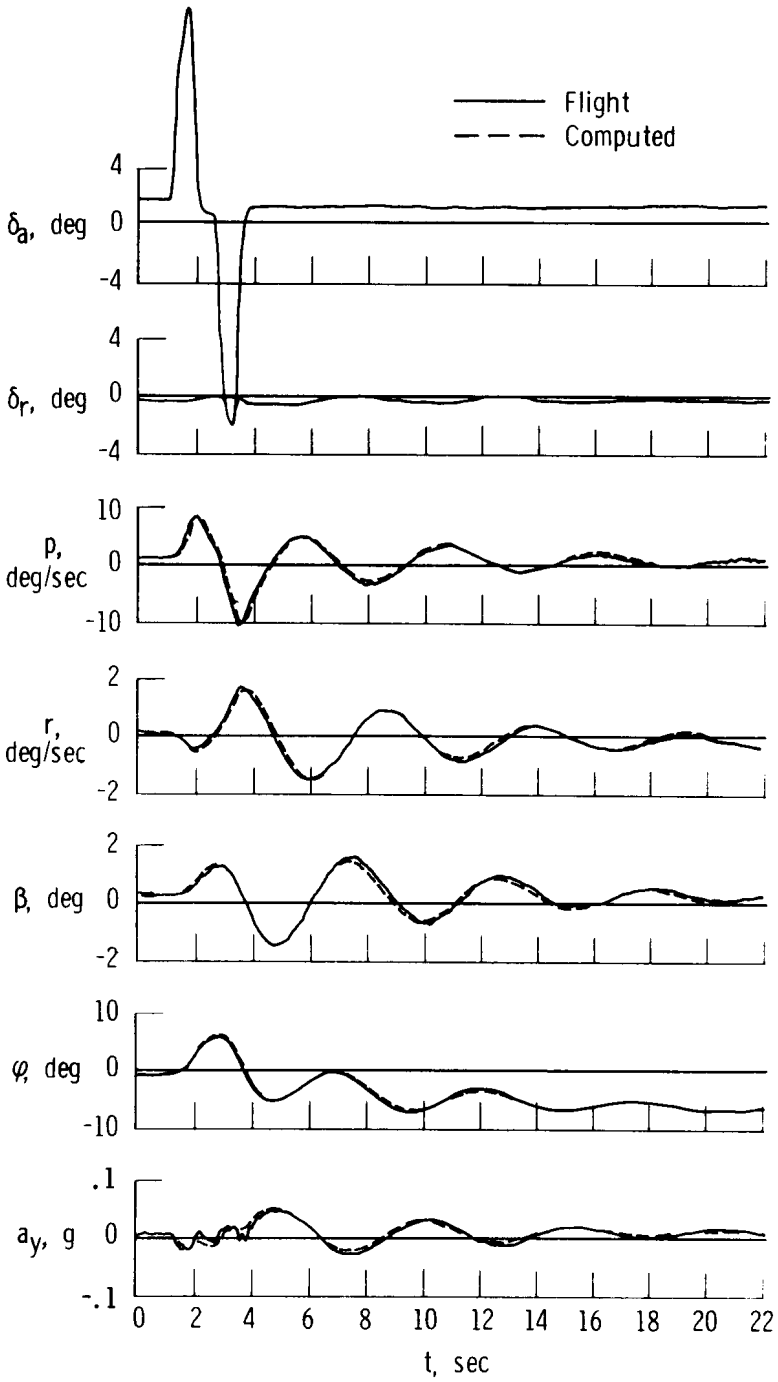

(a) First maneuver.

Figure 21. Comparison of the XB-70 time histories measured in flight and computed by using coefficients obtained from flight data with the modified Newton-Raphson method without a priori weighting. K = 0.

history in figure 20(a), so these values had to be fixed at some a priori value while the estimates were obtained. A similar situation exists for L_{δ_a}, N_{δ_a}, and Y_{δ_a} in the time history of figure 20(b). The net result of these techniques is a different set of control derivatives for two maneuvers known to be at the same flight condition. This could be alleviated rather laboriously by repeating the procedure several times, each time updating with the most recently obtained control derivative.

The problem can be eliminated with the Newton-Raphson method by recognizing in equation (14) that the summations may be continued for more points if corrections are made for the initial conditions at each of the discontinuities where a new time history is started. This method was used to obtain the comparison of flight data with data computed by using the Newton-Raphson method without a priori weighting in figures 21(a) and 21(b). The match is considered to be good, and little could be suggested to improve it.

Figures 22(a) and 22(b) compare the two flight time histories with the computed time histories based upon the estimates obtained by the Newton-Raphson method with the a priori weighting set at K = 80. The fit would still be considered good, although some phase shift is now apparent, particularly in the r, β, and a_y traces.

Figure 23 is a summary of the estimates obtained by using

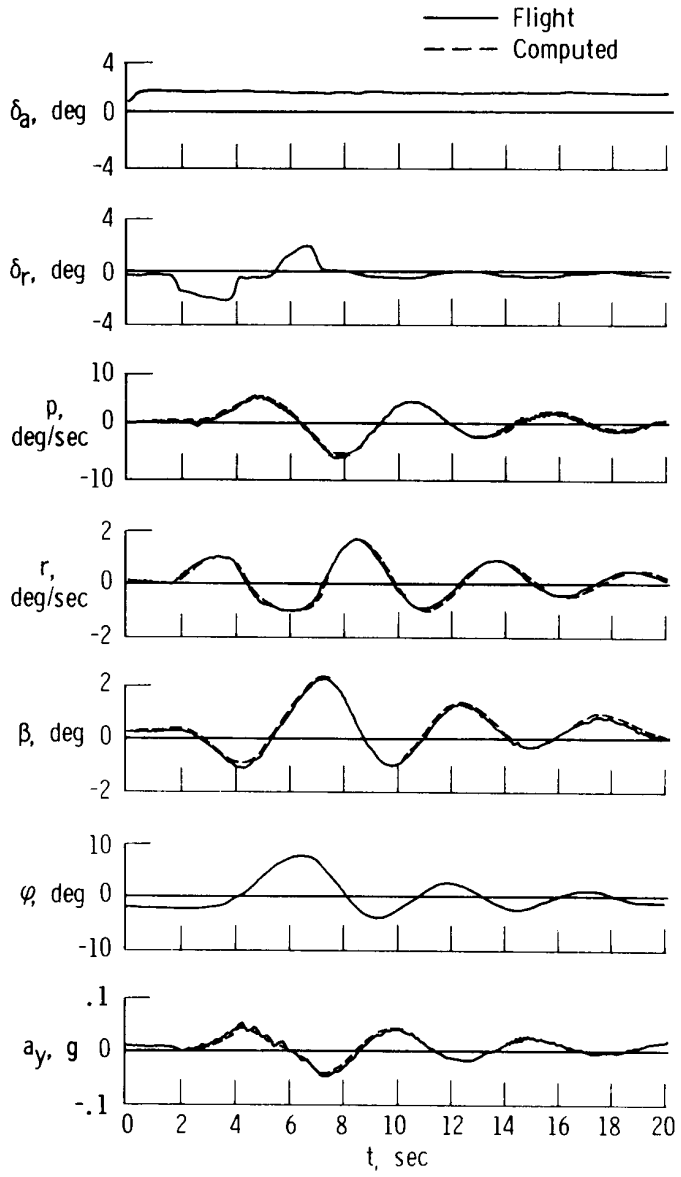

(b) Second maneuver.

Figure 21. Concluded.

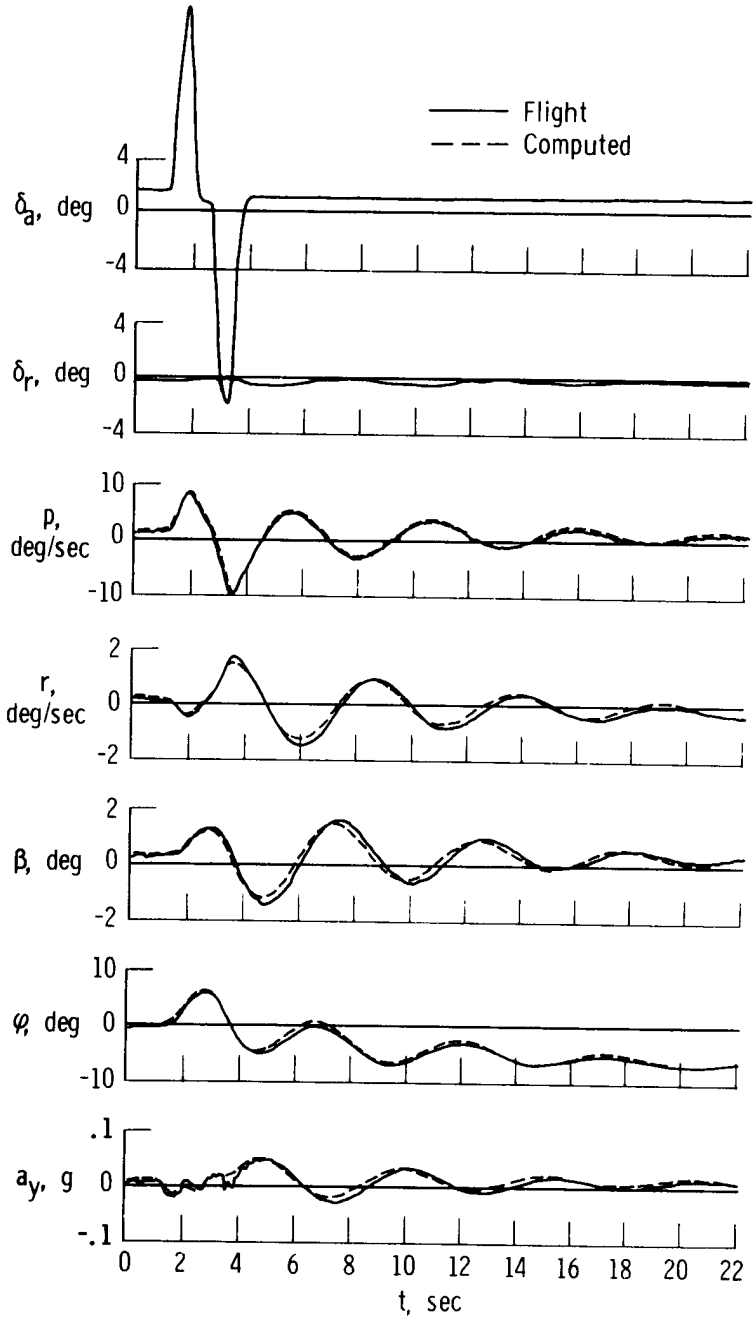

(a) First maneuver.

Figure 22. Comparison of the XB-70 time histories measured in flight and computed by using coefficients obtained from flight data with the modified Newton-Raphson method with an a priori weighting which doubles the unweighted fit error. K = 80.

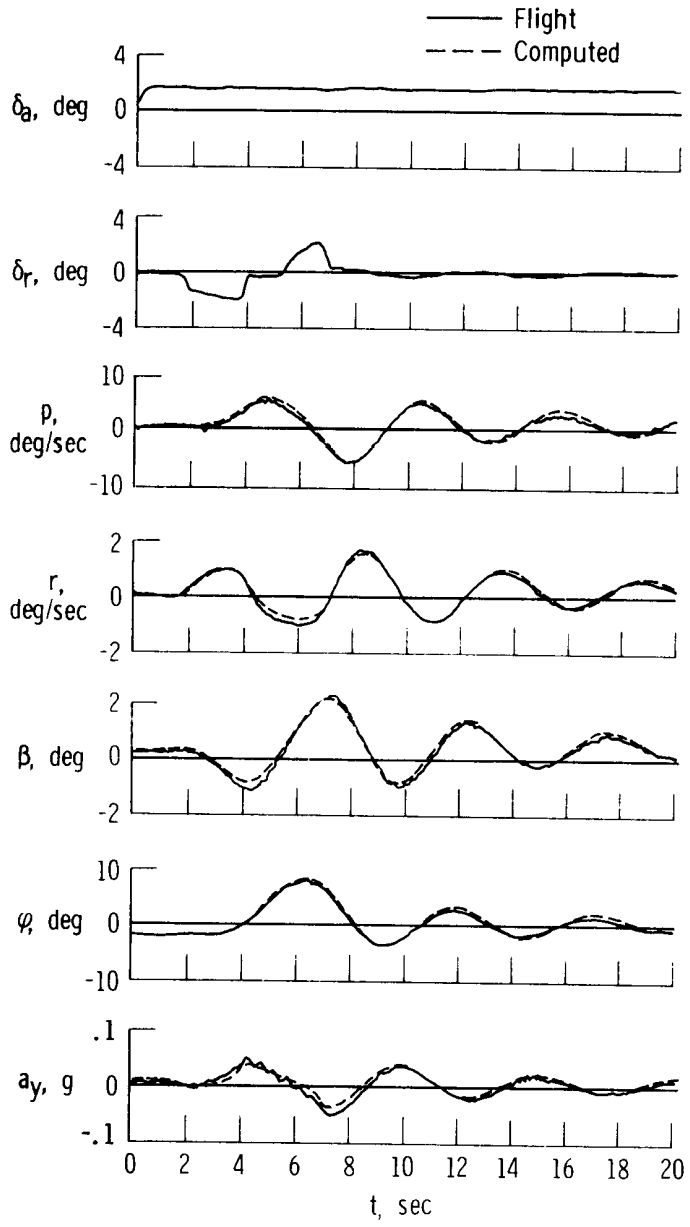

(b) Second maneuver.

Figure 22. Concluded.

the three different methods. It is significant that L_p, L_{δ_a}, N_β, N_{δ_r}, Y_p, and Y_β are approximately the same for all three methods, but L_β, L_{δ_r}, and N_{δ_a} are relatively unaffected by the a priori weighting. In contrast, in figure 13 for the X-15 airplane it was noted that N_{δ_a} was readily changed to the a priori value and in figure 19 for the light airplane L_{δ_r} was easily changed to equal the a priori value. Thus, different combinations of derivatives appear to be strong or weak for each maneuver analyzed.

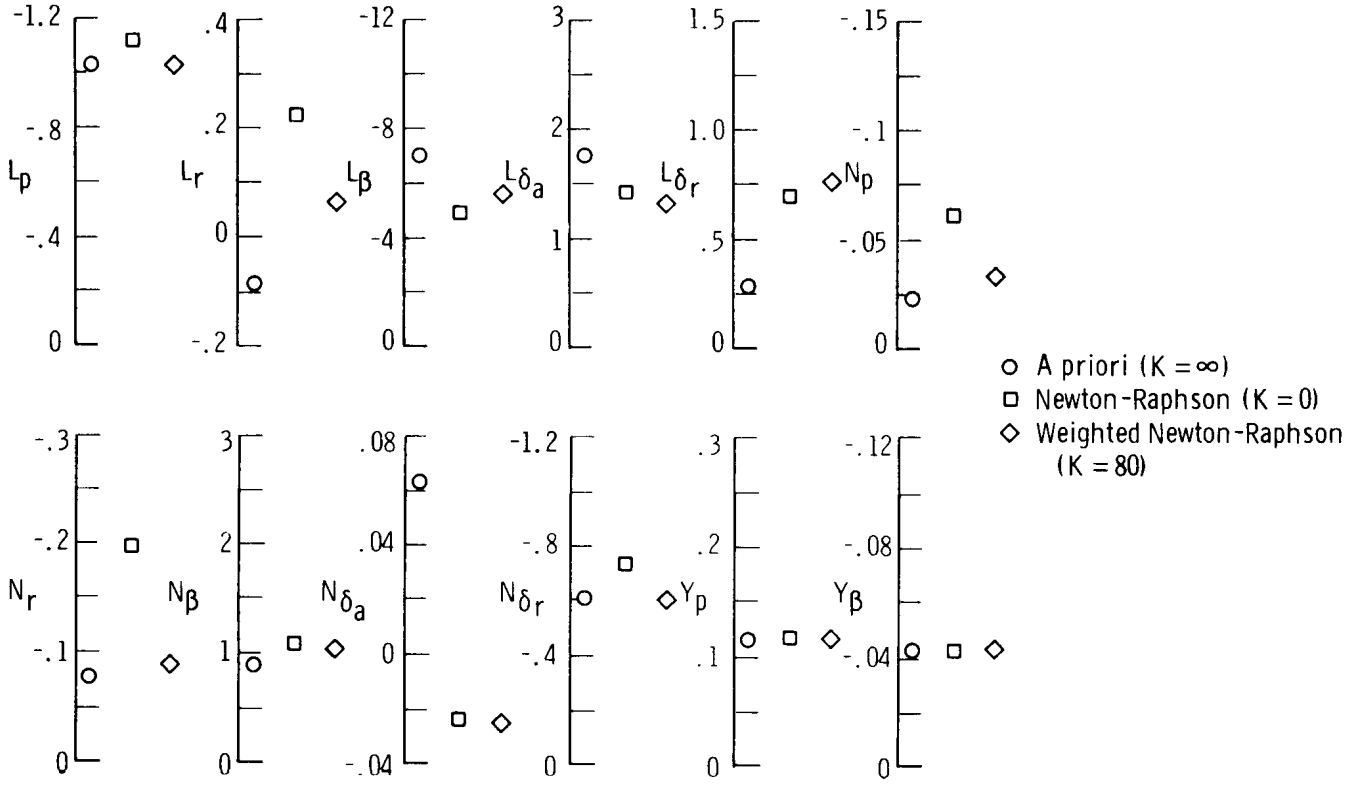

Figure 23. Comparison of XB-70 coefficients determined from flight data by using a modified Newton-Raphson method and from a priori values.

Lifting Body Vehicles

Lifting body reentry vehicles (ref. 15) represent a wingless aircraft with somewhat unusual aerodynamic characteristics. The lifting body maneuver selected for analysis is a combination aileron and rudder maneuver.

Figure 24 is a comparison of time histories obtained from flight data and computed from the predictions based upon wind-tunnel (a priori) estimates. The $\dot{p}$ and $\dot{r}$ signals were not measured. The drift of the computed signals is severe, probably largely because of biases in the control measurements.

Figure 25 compares flight data with data computed by using the Newton-Raphson method without a priori weighting. The fit is good on p, φ, and a_y, but there is some phase shift in r and β.

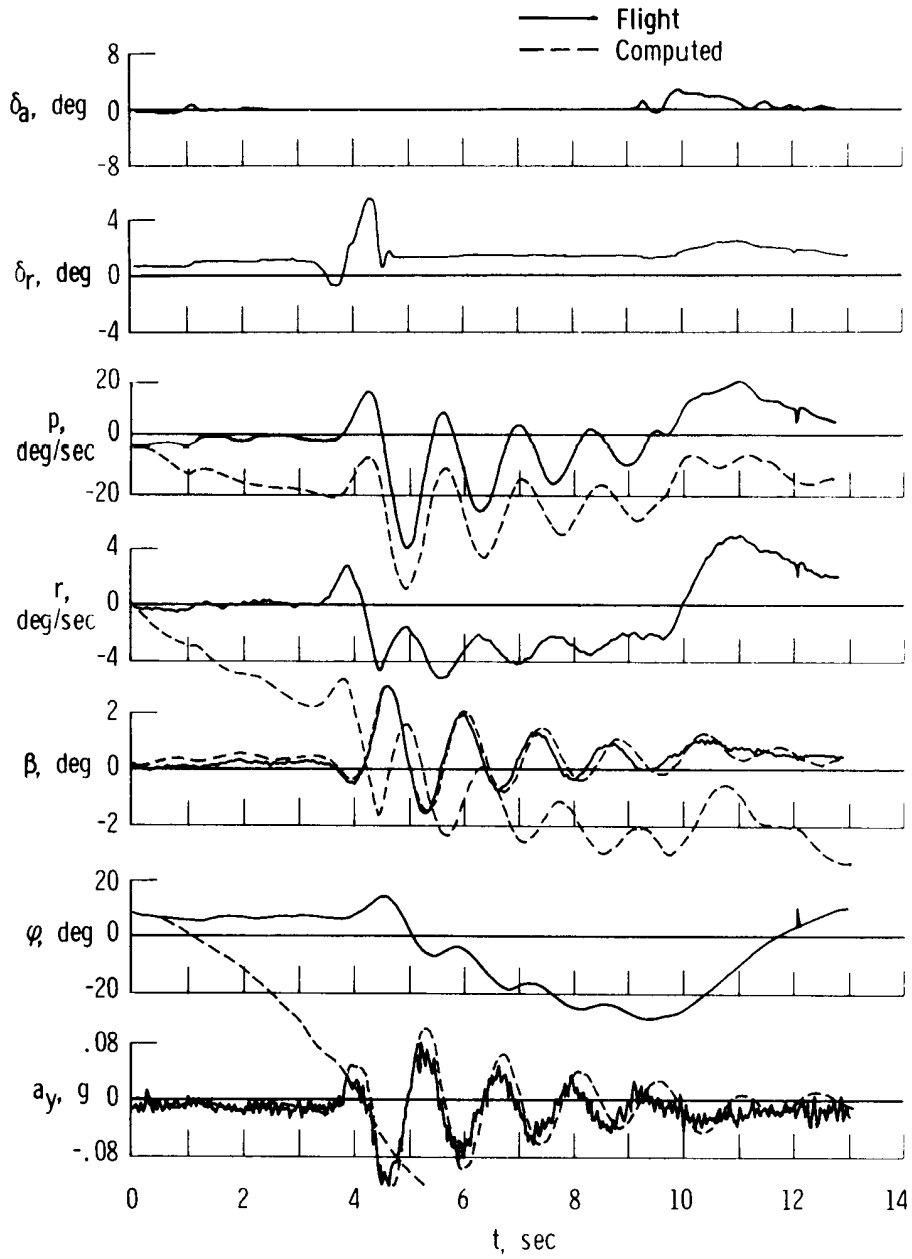

Figure 24. Comparison of lifting body vehicle time histories measured in flight and computed by using a priori values. $K = \infty$.

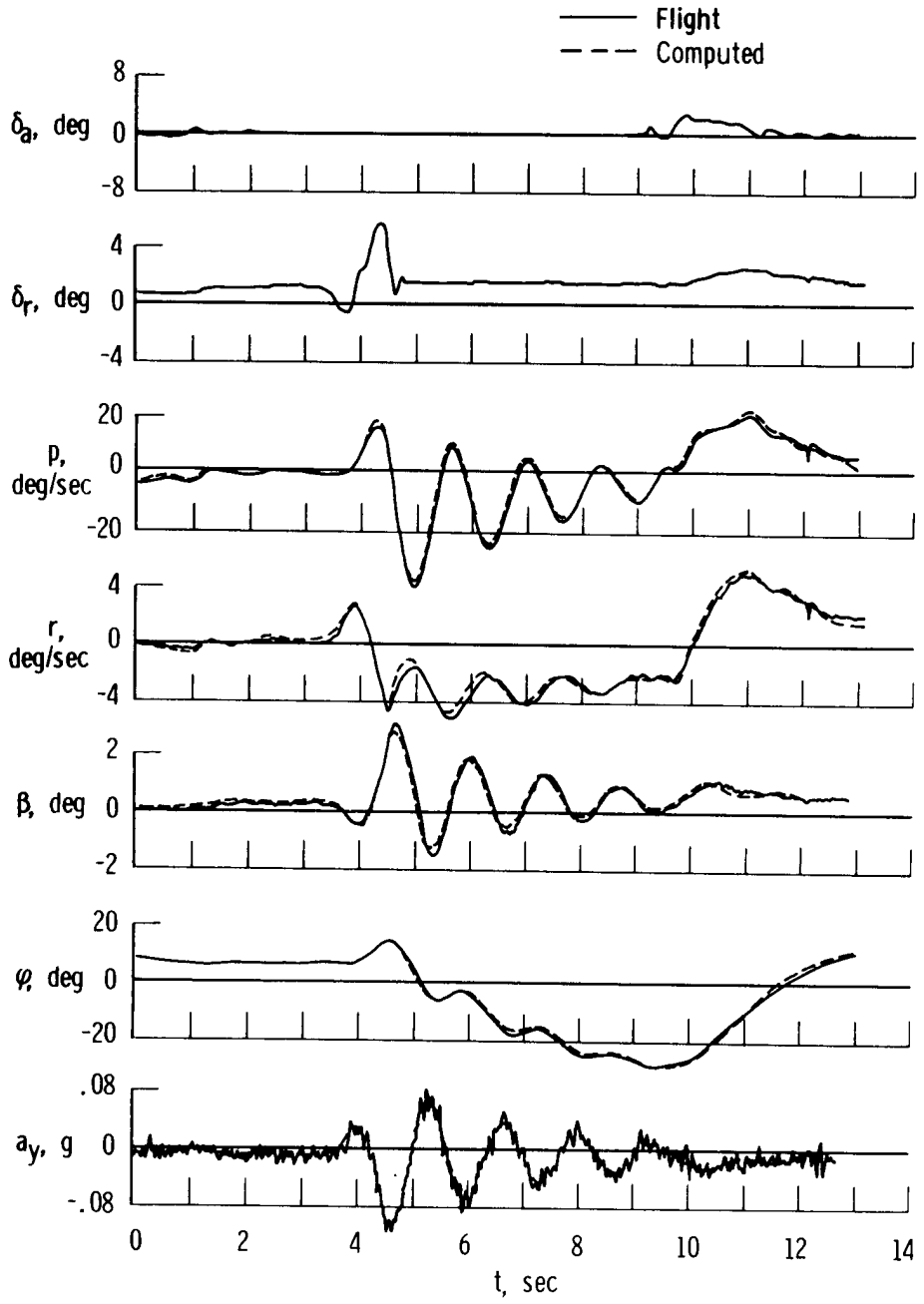

Figure 25. Comparison of lifting body vehicle time histories measured in flight and computed by using coefficients obtained from flight data with the modified Newton-Raphson method without a priori weighting. K = 0.

In figure 26 flight data are compared with data computed by using the Newton-Raphson method with an a priori weighting of K = 22. The fit is still fairly good, but some of the maximum excursions fail to match.

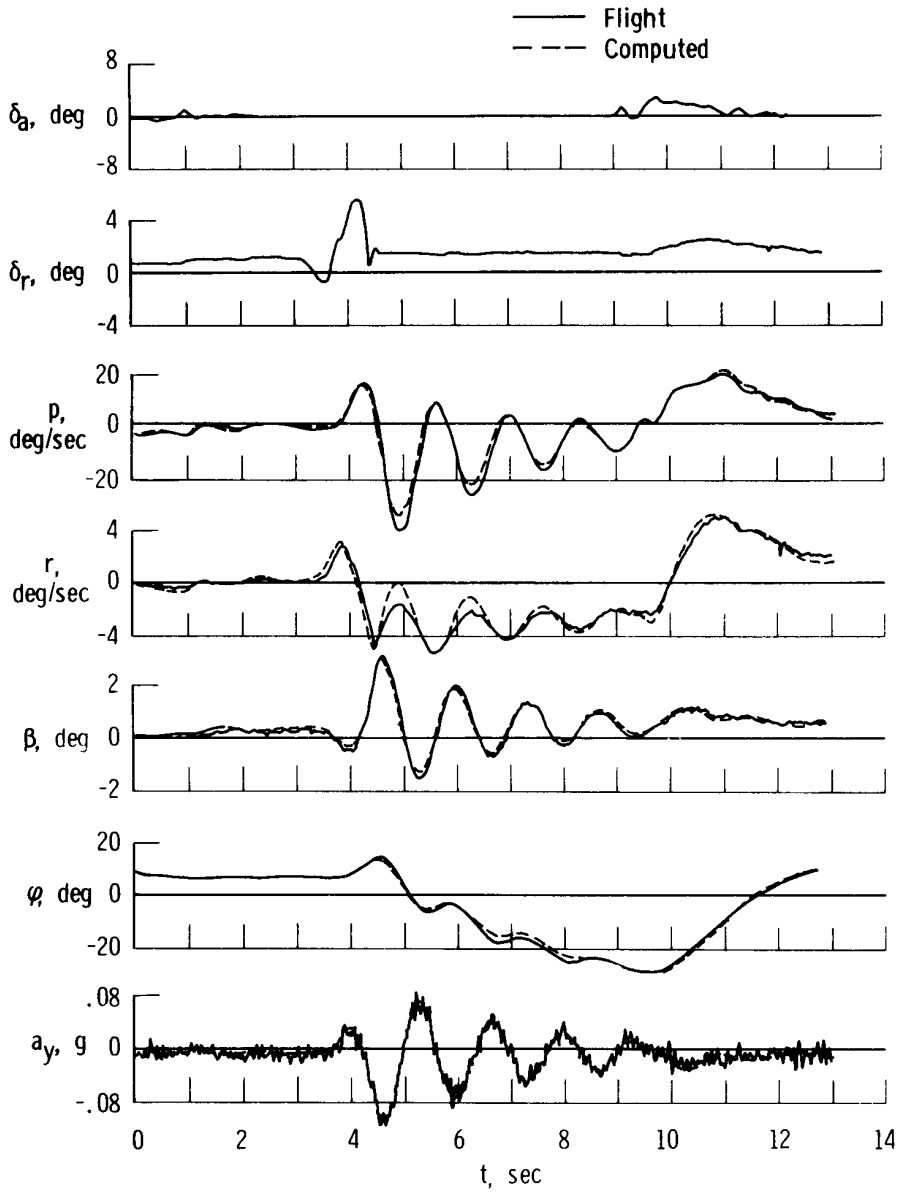

Figure 26. Comparison of lifting body vehicle time histories measured in flight and computed by using coefficients obtained from flight data with the modified Newton-Raphson method with an a priori weighting which doubles the unweighted fit error. K = 22.

Figure 27 is a summary of the coefficient estimates obtained by using the three methods. For this vehicle L_p, L_β, N_β, N_{δ_r}, Y_p, and Y_β are approximately the same for all three methods. The coefficients N_p and N_{δ_a} appear to remain near the unweighted estimates in spite of the weighting.

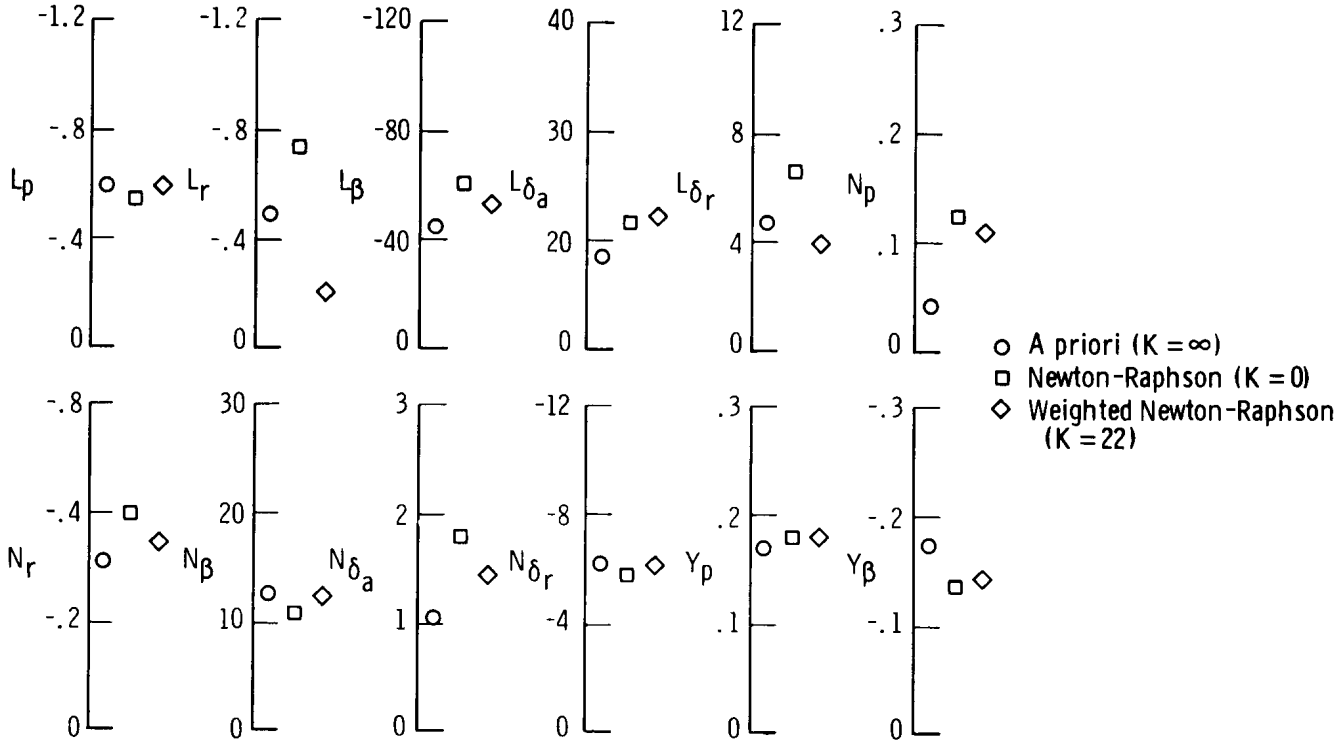

Figure 27. Comparison of lifting body vehicle coefficients determined from flight data by using a modified Newton-Raphson method and from a priori values.

Summary of Results for Various Vehicles

Even though the same relative weighting in the D_2 matrix was used for all four vehicles, different coefficients in each case are affected by that same weighting. Although this does not indicate that the D_2 matrix is adequate, it does show that the information in the data primarily determines the estimate of the coefficient. This is a desirable characteristic of the technique, inasmuch as it departs from the a priori value only if the measured data contain information contradictory to the a priori coefficients.

In summary, the application of the Newton-Raphson method to the four vehicles resulted in (1) a good fit of the computed data with the flight data, (2) a set of reasonable derivatives, and (3) the a priori option which indicated the coefficients to place confidence in.

APPLICATION TO SHORT-PERIOD LONGITUDINAL MODE

With $\dot{x} = Ax + Bu$ and $y = \left[\frac{I}{G}\right]x + \left[\frac{I}{H}\right]u$ as the constant coefficient differential

equation, the Newton-Raphson method was used on the so-called short-period longitudinal aircraft mode where

$$\mathbf{u} = \begin{bmatrix} \delta_e \\ \delta_0 \end{bmatrix} \qquad \mathbf{x} = \begin{bmatrix} q \\ \alpha \\ V \\ \Theta \end{bmatrix} \qquad \dot{\mathbf{x}} = \begin{bmatrix} \dot{q} \\ \dot{\alpha} \\ \dot{V} \\ \dot{\Theta} \end{bmatrix} \qquad \mathbf{y} = \begin{bmatrix} \frac{x}{\dot{q}} \\ a_z \\ a_x \end{bmatrix}$$

$$A = \begin{bmatrix} M_q & M_\alpha & M_V & 0 \\ Z_q & Z_\alpha & Z_V & Z_\Theta \\ X_q & X_\alpha & X_V & X_\Theta \\ 1 & 0 & 0 & 0 \end{bmatrix} \qquad B = \begin{bmatrix} M_{\delta_e} & M_{\delta_0} \\ Z_{\delta_e} & Z_{\delta_0} \\ X_{\delta_e} & X_{\delta_0} \\ 0 & 0 \end{bmatrix}$$

$$G = \begin{bmatrix} M_q & M_\alpha & M_V & 0 \\ 0 & Z_\alpha & 0 & 0 \\ 0 & X_\alpha & 0 & 0 \end{bmatrix} \qquad H = \begin{bmatrix} M_{\delta_e} & M_{\delta_0} \\ Z_{\delta_e} & Z_{\delta_0} \\ X_{\delta_e} & X_{\delta_0} \end{bmatrix}$$

The coefficients in G and H are also in A and B. Because only the short-period mode was analyzed, only the elements of the first two rows and columns of the A and B matrices and the biases on the state variables q and α were variable.

The XB-70 (ref. 14) flight data were used for this part of the analysis. Figure 28 is a comparison of the flight-measured data and data computed from the wind-tunnel predicted (a priori) estimates. Only the q, α, $\dot{q}$, and a_z signals were used, and the corresponding elements in the D_1 (table 2) matrix were set to zero for the other signals. The fit is fairly good, although some departure is noted in all the signals.

Figure 29 compares the flight data with the data computed by using the coefficients obtained from the Newton-Raphson method without a priori weighting. The fit is extremely good for all the signals; very little could be suggested to improve it.

Figure 30 compares the flight data with the computed time history based on coefficients obtained with the Newton-Raphson method with an a priori weighting of K = 0.03. The fit is still good, but the q signal shows a small departure near the maximum excursions. The coefficients are now weighted toward the a priori prediction, thus this is a satisfactory compromise.

The coefficients obtained by the three methods are summarized in figure 31. The coefficients agree well except for M_q, M_{δ_e}, and Z_{δ_e}. The a priori weighting tends to bring these quantities toward the wind-tunnel values. The initial peak on a_z and $\dot{q}$ in figure 28 showed the computed values to be larger, so it is obvious that the data contain information contrary to the wind-tunnel values. One apparent advantage in determining a smaller number of unknowns is that a visual interpretation of the time histories can be maintained for the effect of each of the coefficients. This gives some confidence that the a priori feature of this method is performing the same function for more unknowns.

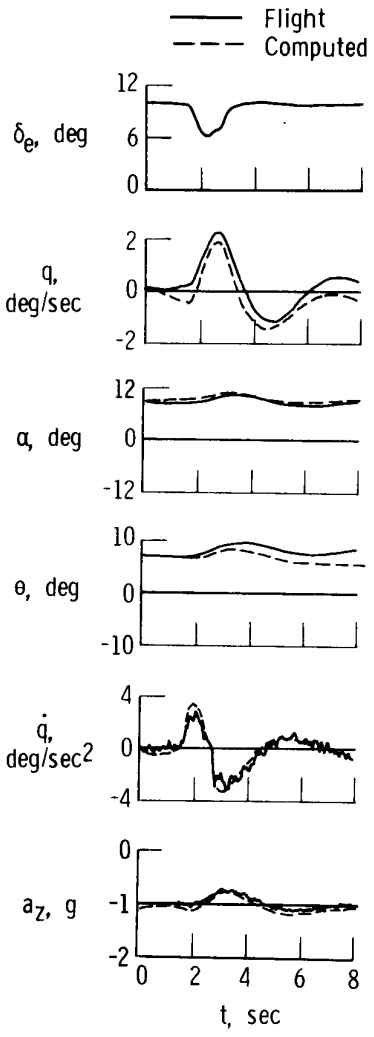

Figure 28. Comparison of XB-70 longitudinal time histories measured in flight and computed by using a priori values. $K = \infty$.

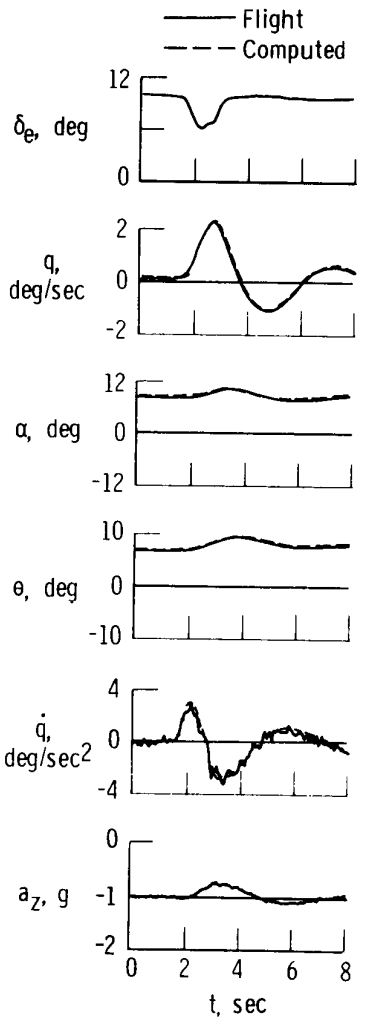

Figure 29. Comparison of XB-70 longitudinal time histories measured in flight and computed by using coefficients obtained from flight data with the modified Newton-Raphson method without a priori weighting.

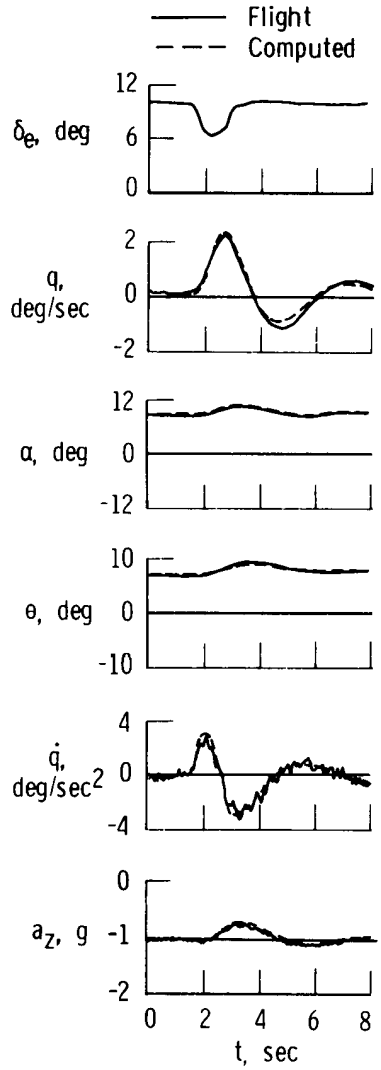

Figure 30. Comparison of XB-70 longitudinal time histories measured in flight and computed by using coefficients obtained from flight data with the modified Newton-Raphson method with an a priori weighting which doubled the unweighted fit error. K = 0.03.

IMPROVING MANEUVERS

In future studies of coefficient determination, better maneuvers should be defined in order to maximize the amount of information contained in the data. The data analyzed in this report were generated specifically for existing analysis techniques. This generally entailed separating data into various segments, such as one in which only one control was moving and another with no input so the zero input dynamics appeared clearly. Because the stability and control coefficients are needed for sophisticated research vehicles which only briefly maintain a given flight condition, these types of maneuvers are difficult to obtain.

Heuristically, certain types of maneuvers can be defined that would increase the information content of the data. If no a priori information about the coefficients were available, white noise would be desirable as the control input to insure that all frequencies were represented in the input. Knowledge of the coefficients implicitly provides knowledge of the frequency of the modes being investigated. It might be assumed that the control input should resemble a frequency sweep in the frequency range of interest. In addition, the amplitude of the resultant maneuver should be in the linear range of the coefficients, but the motions should be large to minimize the effect of the noise. In summary, intuition suggests a frequency-sweep control input,

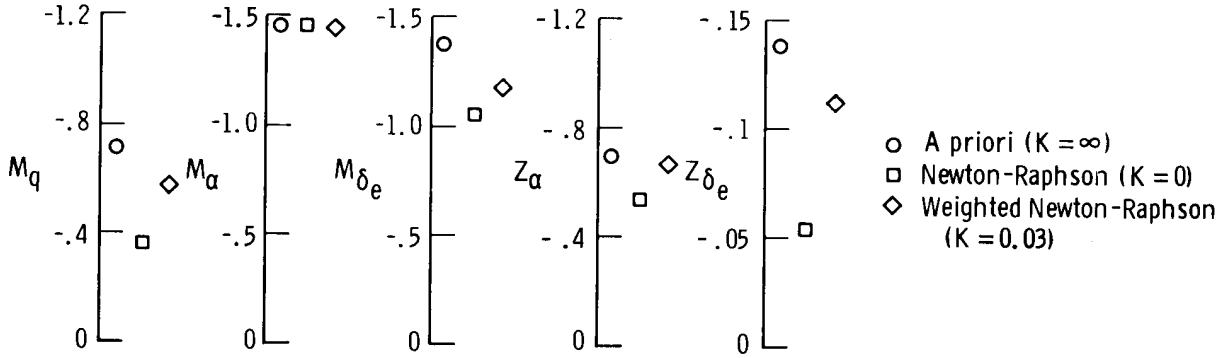

Figure 31. Comparison of XB-70 longitudinal coefficients determined from flight data by using a modified Newton-Raphson method and from a priori values.

large motion in the maneuver, and linear responses.

CONCLUDING REMARKS

Stability derivatives or coefficients of the state equations were determined by using several methods. An example set of X-15 lateral-directional flight data was analyzed by using simplified-equations, analog-matching, least-squares, and Shinbrot methods. The same set of flight data was analyzed by using a gradient method to find the set of coefficients that would minimize the integral-squared error between the measured state and that computed by using the coefficients obtained with the same control input. Difficulties in convergence were encountered when there were more than a few unknowns.

A modified Newton-Raphson (quasi-linearization) method of minimization was used with success to solve the convergence problem. The resulting fit of the flight data was clearly superior to that of the least-squares and Shinbrot methods. One important advantage of the Newton-Raphson method is that it is not necessary that all components of the state variables and their time derivatives be measured.

The use of a priori values (for example, values predicted from wind-tunnel data) in the Newton-Raphson method resulted in estimates that made full use of all available information. When the a priori option was used, the coefficients that were only weakly determined by using only flight data approached their a priori values and the fit error increased slightly. This was found to be an effective way of utilizing previously analyzed data together with new data to update the estimates of the coefficients.

A model statistically similar to the flight data was constructed and used, and the values for the coefficients were determined by using the least-squares, Shinbrot, and Newton-Raphson methods. The Newton-Raphson method was superior to all other methods for the example considered.

An expression was derived with the Cramèr-Rao inequality to obtain a bound for the error covariance matrix for an idealized case. The results of this bound were compared with the variances obtained from the statistical model. The Cramèr-Rao bound was found to give insight into the reliability of the estimates obtained with the modified Newton-Raphson method.

To demonstrate that the Newton-Raphson method was generally applicable to a wide range of modern aircraft, it was applied also to a light general aviation airplane, a large supersonic airplane, and a lifting body vehicle. The method proved to be satisfactory for each of the maneuvers analyzed and for two maneuvers made at the same flight condition which were analyzed simultaneously.

The Newton-Raphson technique was applied to longitudinal equations of motion of an airplane and was found to be successful for the short-period longitudinal mode analyzed.

To obtain better estimates of the coefficients of the state equations more research is needed to define the weighting matrices used in the cost functionals and the types of maneuvers needed to maximize the information contained in the data.

Flight Research Center,
National Aeronautics and Space Administration,
Edwards, Calif., October 4, 1971.

APPENDIX

CRAMÈR-RAO BOUND

In an identification problem it is useful to have a bound on the error covariance matrix. By making several assumptions about the noise and the estimates of the coefficients, some indication of the reliability of the estimates can be obtained by applying the Cramèr-Rao inequality (ref. 5). By assuming the noise to be Gaussian and defining an extended noise vector, $\mathbf{n}_e$, formed by stacking subsequent $(R \times 1)$ noise vectors sequentially with increasing time, the probability density function can be represented as

$$\rho(\mathbf{n}_e) = \frac{1}{2\pi^{\frac{R}{2}m} |W|^{1/2}} \; e^{-1/2\left[\mathbf{n}_e^T W^{-1} \mathbf{n}_e\right]}$$

where

$$\mathbf{n}_e = \begin{bmatrix} \mathbf{n}^1 \\ \mathbf{n}^2 \\ \vdots \\ \mathbf{n}^{l-1} \\ \mathbf{n}^l \end{bmatrix}$$

and the superscript i represents the time of the sample, l is the total number of samples, and W is the covariance matrix of the noise, $\mathbf{n}_e$.

For the noise, $\mathbf{n}_e = \mathbf{z}_e - \mathbf{y}_e$, the conditional probability density function can easily be shown to be

$$\rho(\mathbf{z}_e \mid \mathbf{c}_T) = \frac{1}{2\pi^{\frac{R}{2}m} |W|^{1/2}} \; e^{-1/2\,(\mathbf{z}_e - \mathbf{y}_e)^T W^{-1} (\mathbf{z}_e - \mathbf{y}_e)}$$

where $\mathbf{z}_e$ is the sampled data vector and $\mathbf{y}_e$ is the sampled true state vector as follows:

$$\mathbf{z}_e = \begin{bmatrix} \mathbf{z}^1 \\ \mathbf{z}^2 \\ \vdots \\ \mathbf{z}^{l-1} \\ \mathbf{z}^l \end{bmatrix} \qquad \mathbf{y}_e = \begin{bmatrix} \mathbf{y}^1 \\ \mathbf{y}^2 \\ \vdots \\ \mathbf{y}^{l-1} \\ \mathbf{y}^l \end{bmatrix}$$

and where $\mathbf{c}_T$ is the true value of the estimate and the superscript i represents the time index of the sample. If, in addition, the estimate of $\mathbf{c}$ is assumed to be asymptotically unbiased, the Cramèr-Rao bound can be written as

$$\Phi = E\left\{(\mathbf{c} - \mathbf{c}_T)(\mathbf{c} - \mathbf{c}_T)^T\right\}$$

$$\geq \left\{ E\left\{ \left[\nabla_{\mathbf{c}} \log \rho(\mathbf{z}_e \mid \mathbf{c}_T)\right]^T \left[\nabla_{\mathbf{c}} \log \rho(\mathbf{z}_e \mid \mathbf{c}_T)\right] \right\} \right\}^{-1}$$

where the expectation $E\{\cdot\}$ is with respect to $\mathbf{z}_e$

$$= \left\{ E\left[\nabla_{\mathbf{c}}\, \mathbf{y}_e{}^T\, W^{-1^T} (\mathbf{z}_e - \mathbf{y}_e)(\mathbf{z}_e - \mathbf{y}_e)^T W^{-1} \nabla_{\mathbf{c}}\, \mathbf{y}_e \right] \right\}^{-1}$$

Substituting $\mathbf{n}_e = \mathbf{z}_e - \mathbf{y}_e$,

$$= \left\{ E\left[\nabla_{\mathbf{c}}\, \mathbf{y}_e{}^T W^{-1^T} \mathbf{n}_e \mathbf{n}_e{}^T W^{-1} \nabla_{\mathbf{c}}\, \mathbf{y}_e \right] \right\}^{-1}$$

By further assuming that the noise is also white, the representation for W^{-1} becomes block diagonal such that

$$W^{-1} = \begin{bmatrix} D^1 & 0 & 0 & \cdots & 0 & 0 \\ 0 & D^2 & 0 & \cdots & 0 & 0 \\ 0 & 0 & D^3 & \cdots & 0 & 0 \\ \vdots & \vdots & \vdots & \ddots & \vdots & \vdots \\ 0 & 0 & 0 & \cdots & D^{l-1} & 0 \\ 0 & 0 & 0 & \cdots & 0 & D^{l} \end{bmatrix}$$

where D^i is $(R \times R)$ and W is $(\ell R \times \ell R)$. With this assumption the last equation simplifies to

$$\Phi \geq \left\{ E\left[\sum_{i=1}^{\ell} \nabla_c \left[y^i \right]^T D^{iT} n^i n^{iT} D^i \nabla_c \left[y^i \right] \right] \right\}^{-1}$$

Interchanging the summation with the expected value and noting that only the noise n^i is a function of z^i,

$$\Phi \geq \left\{ \sum_{i=1}^{\ell} \nabla_c \left[y^i \right]^T D^{iT} E\left\{ n^i n^{iT} \right\} D^i \nabla_c \left[y^i \right] \right\}^{-1}$$

Noting for the assumption of white noise that

$$E\left\{ n^i n^{iT} \right\} = \left[D^i \right]^{-1}$$

then

$$\Phi \geq \left\{ \sum_{i=1}^{\ell} \nabla_c \left[y^i \right]^T D^i \nabla_c \left[y^i \right] \right\}^{-1}$$

If, in addition, stationarity of the noise is assumed, then

$$D = D^i = D^j \quad \text{for all } i \text{ and } j$$

Thus, the desired result for the matrix Cramèr-Rao bound, Φ, of the error covariance matrix becomes

$$\Phi \geq \left\{ \sum_{i=1}^{\ell} \nabla_c \left[y^i \right]^T D^T \nabla_c \left[y^i \right] \right\}^{-1}$$

REFERENCES

1. Wolowicz, Chester H.: Considerations in the Determination of Stability and Control Derivatives and Dynamic Characteristics From Flight Data. AGARD Rep. 549-Part 1, 1966.

2. Rampy, John M; and Berry, Donald T.: Determination of Stability Derivatives From Flight Test Data by Means of High Speed Repetitive Operation Analog Matching. FTC-TDR-64-8, Air Force Flight Test Center, May 1964.

3. Howard, J.: The Determination of Lateral Stability and Control Derivatives From Flight Data. Canadian Aeronautics and Space Journal, vol. 13, March 1967, pp. 127-134.

4. Shinbrot, Marvin: On the Analysis of Linear and Nonlinear Dynamical Systems From Transient-Response Data. NACA TN 3288, 1954.

5. Balakrishnan, A. V., ed.: Communication Theory. McGraw-Hill Book Co., c. 1968.

6. Bellman, Richard E.; and Kalaba, Robert E.: Quasilinearization and Nonlinear Boundary-Value Problems. American Elsevier Publishing Company, Inc., 1965.

7. Mechtly, E. A.: The International System of Units - Physical Constants and Conversion Factors. NASA SP-7012, 1969.

8. Anon.: Dynamics of the Airframe. Bu. Aer. Rep. AE-61-4 II, Northrop Corp., Norair Div., Sept. 1952.

9. DeRusso, Paul M.; Roy, Rob J.; and Close, Charles M.: State Variables for Engineers. John Wiley & Sons, Inc., c. 1965.

10. Yancey, Roxanah B.: Flight Measurements of Stability and Control Derivatives of the X-15 Research Airplane to a Mach Number of 6.02 and an Angle of Attack of 25°. NASA TN D-2532, 1964.

11. Powell, M. J. D.: A Survey of Numerical Methods for Unconstrained Optimization. Studies in Optimization 1, Soc. for Industrial and Applied Math., c. 1970, pp. 43-61.

12. Anon.: SDS 9300 Computer Reference Manual. 90 00 50E, Scientific Data Systems, July 1966.

13. Fink, Marvin P.; and Freeman, Delma C., Jr.: Full-Scale Wind-Tunnel Investigation of Static Longitudinal and Lateral Characteristics of a Light Twin-Engine Airplane. NASA TN D-4983, 1969.

14. Andrews, William H.: Summary of Preliminary Data Derived From the XB-70 Airplane. NASA TM X-1240, 1966.

15. McTigue, John G. ; and Ryan, Bertha M. : Lifting-Body Research Vehicles in a Low-Speed Flight Test Program. Annals of the New York Academy of Sciences, vol. 154, art. 2, Nov. 22, 1968, pp. 1014-1032.

NASA-Langley, 1972 —— 19 H-626